



UNIVERSITY OF THESSALY
DEPARTMENT OF ELECTRICAL AND COMPUTER ENGINEERING

DIPLOMA THESIS

Study and Analysis of Electric Motors

Author:
Konstantinos Prantikos

Supervisor:
Professor George Stamoulis

*A Thesis submitted in fulfillment of the requirements
for the degree of Diploma
in the
Department of Electrical and Computer Engineering*

Volos, March 2019

Μελέτη και ανάλυση ηλεκτρικών κινητήρων

Κωνσταντίνος Πραντικός

Περίληψη

Σκοπός της παρούσας διπλωματικής εργασίας είναι η μελέτη και ανάλυση δυο ειδών ηλεκτρικών κινητήρων, των κινητήρων επαγωγής και των σύγχρονων κινητήρων μονίμων μαγνητών. Αρχικά πραγματοποιήθηκε βιβλιογραφική διερεύνηση των δυνατοτήτων και των επιλογών που υπάρχουν αναφορικά με τη χρήση ηλεκτρικών κινητήρων σε οχήματα. Μετά από μία σύντομη παρουσίαση του ηλεκτροκίνητου οχήματος ως εφαρμογή, ακολουθεί η ανάλυση του κινητήρα ως βασικού υποσυστήματος του και αντικειμένου μελέτης αυτής της εργασίας.

Πρώτα μελετήθηκε και αναλύθηκε ο κινητήρας επαγωγής. Παρουσιάστηκε η δομή του κινητήρα και αναλύθηκαν στοιχεία της κατασκευής όπως ο στάτης, ο δρομέας και τα τυλίγματα. Στην συνέχεια αναλύθηκε η αρχή λειτουργίας καθώς και το ισοδύναμο κύκλωμα του κινητήρα, ενώ αναλύθηκαν οι αντιστροφείς (inverter) και οι τεχνικές ελέγχου του κινητήρα. Πραγματοποιήθηκε προκαταρκτική σχεδίαση με βάση τα μαγνητικά μεγέθη και πεδιακή ανάλυση με πεπερασμένα στοιχεία. Μετά παρουσιάστηκαν οι απώλειες καθώς και οι κατηγορίες των κινητήρων επαγωγής.

Στη συνέχεια μελετήθηκαν και αναλύθηκαν οι σύγχρονοι κινητήρες μονίμων μαγνητών που παρουσιάζουν τάση εξ επαγωγής ημιτονοειδούς και τραπεζοειδούς κυματομορφής. Παρουσιάστηκαν τα υλικά μαγνήτισης καθώς και οι μόνιμοι μαγνήτες που χρησιμοποιούνται στην βιομηχανία. Αναλύθηκε η δομή του κινητήρα μαζί με τις τοπολογίες του δρομέα. Παρουσιάστηκε η αρχή λειτουργίας των κινητήρων, οι αντιστροφείς (inverter) που χρησιμοποιούν και οι τεχνικές ελέγχου τους. Τέλος πραγματοποιήθηκε προκαταρκτική σχεδίαση με βάση τη μελέτη ηλεκτρομαγνητικών φαινομένων που λαμβάνουν χώρα κατά τη λειτουργία ενός ηλεκτρικού κινητήρα.

Λέξεις κλειδιά: κινητήρας επαγωγής, δρομέας κλωβού, κινητήρας μονίμων μαγνητών, τυλίγματα, αντιστροφείς, τεχνικές ελέγχου

UNIVERSITY OF THESSALY
Department of Electrical and Computer Engineering

Diploma Thesis

Study and Analysis of Electric Motors

by Konstantinos Prantikos

Abstract

The aim of this diploma thesis is the study and analysis of two types of electric motors, induction motors and permanent magnet brushless motors. Firstly, a bibliographic search of the possibilities and the choices available regarding the application of electric motors in vehicles was performed. Following the presentation of the electric cars as application, an analysis of the motor is given, as this constitutes a main subsystem of the electric vehicle and it is the focus of this project.

The induction motor was first studied and analyzed. The structure of the motor was presented and structural components such as the stator, the rotor and the windings were analyzed. Then the operating principle and the equivalent motor circuit were analyzed. Also there are presented the inverter topologies and motor control techniques of the motor. A preliminary design based on the magnetic magnitudes and a field analysis with finite elements was performed. The losses were then presented as well as the categories of induction motors.

Two types of permanent magnet brushless motors were then studied and analyzed, the permanent magnet synchronous motors with sinusoidal and trapezoidal waveforms. Magnetic materials as well as permanent magnets used in industry were presented. The structure of the motor was analyzed along with the rotor topology. Their operating principle, inverters and their control techniques were analyzed for both motors. Finally, a preliminary design was carried out based on the study of electromagnetic phenomena occurring during the operation of an electric motor.

Key Words: induction motor, squirrel cage rotor, permanent magnet motor, windings, inverters, control techniques

Acknowledgements

First and foremost, I would like to express my appreciation and deepest gratitude to my advisor, Prof. George Stamoulis, for his continuous support, and motivation. His guidance helped me during my research and writing of this thesis.

Additionally, I am more than thankful to my friends, for all the unforgettable moments we have lived together over the past five years. Our experiences will accompany me throughout my life.

Finally, I would like to thank my family for their supporting, understanding and unwavering belief in me throughout all those years.

CONTENTS

CHAPTER 1 - INTRODUCTION	12
1.1 Motivation	12
1.2 Thesis Structure	12
CHAPTER 2 - ELECTRIC VEHICLES	14
2.1 History of Electric Vehicles	14
2.2 Electric Vehicle drive system	14
2.2.1 Electric Vehicle	15
2.2.2 Hybrid Electric Vehicle	17
2.3 Electric Vehicle Motors	20
2.3.1 Comparative Presentation of Electric Motors	20
2.4 POWER ELECTRONICS	23
2.5 Batteries and Energy Storage Systems	25
2.5.1 Fundamental Characteristics of Batteries	25
2.5.2 Security of EVs and System of Batteries	27
2.5.3 Technology of Batteries	29
2.5.4 Battery Management System (BMS)	32
CHAPTER 3 - INDUCTION MOTORS	36
3.1 Structure of Induction Motors	36
3.1.1 Stator	38
3.1.2 Rotor	40
3.1.3 Windings	41
3.2 Principle of Induction Motors	45
3.3 Modeling of Induction Motor	47
3.4 Inverters for Induction Motors	50
3.4.1 PWM Switching Inverters	51
3.4.2 Soft Switching Inverters	52
3.5 Induction Motor Control	52

3.5.1	Variable Voltage Variable Frequency Control	53
3.5.2	Field Oriented Control	54
3.5.3	Direct Torque Control	55
3.6	Preliminary Design	56
3.6.1	Fundamentals Factors of Dimensioning	56
3.6.2	Steps of Preliminary Design	58
3.7	Field Analysis with Finite Elements	60
3.7.1	Magneto-static problems	61
3.7.2	Boundary Conditions	62
3.7.3	The Finite Element Method	64
3.7.4	Finite Element Analysis using the FEMM program	64
3.8	Copper Losses	64
3.9	Core Losses	65
3.9.1	Hysteresis Losses	65
3.9.2	Eddy Current Losses	66
3.10	Induction Motor Classes	67
CHAPTER 4 - PERMANENT MAGNET BRUSHLESS MOTORS		73
4.1	Permanent Magnet Materials	73
4.2	Permanent Magnets	76
4.3	Operating Point and Air Gap Line	78
4.4	Effect of External Magnetic Field Intensity	81
4.5	Arrangement of Permanent Magnets	82
4.6	Magnetization of Permanent Magnets	83
4.7	Structure of Permanent Magnet Brushless Motors	85
4.7.1	Permanent Magnet Rotor Types	85
4.8	Winding	88
4.9	Losses	88
4.10	Types of PM brushless motors	89

4.11	Permanent Magnet Synchronous Motor	89
4.11.1	Principle of PMSM	89
4.11.2	Inverter of PMSM	90
4.11.3	Control of PMSM	91
4.12	Permanent Magnet Brushless DC Motor	92
4.12.1	Principle of BLDC	92
4.12.2	Inverter of BLDC	93
4.12.3	Control of BLDC	93
4.12.4	Position Sensor for BLDC	94
4.13	Preliminary Design	97
4.13.1	Field Factors	98
4.13.2	Performance	99
4.13.3	Torque Ripple	100
4.13.4	Cogging Torque	100
4.13.5	Short-circuiting Current	101
4.13.6	Resistance of Stator Windings	101
4.13.7	Friction and Wind Losses	103
4.13.8	Calculation of Motor Efficiency Coefficient	104
CHAPTER 5 - CONCLUSION		106
5.1	Conclusion	106
5.2	Future Work	106
BIBLIOGRAPHY		107

List of Figures

2.1	Drive system of an electric vehicle	15
2.2	Components of electric vehicle's drive system	17
2.3	HEV series configuration	18
2.4	HEV parallel configuration	19
2.5	HEV series-parallel configuration	19
2.6	PHEV configuration	20
2.7	Induction Motor	21
2.8	Permanent Magnet Motor	22
2.9	Synchronous Reluctance Motor	22
2.10	Principle of power electronic converter	24
2.11	Battery pack of a Tesla Model S electric vehicle	27
2.12	Complete storage system of batteries of GM's electric vehicle	28
2.13	Diagram of Battery Management System (BMS)	32
3.1	Structure diagram of Induction motor	37
3.2	Topology of induction motor	37
3.3	Outer-rotor induction motor topology	38
3.4	Stator of induction motor	39
3.5	Asymmetrical magnetic attraction	40
3.6	Squirrel cage rotor with skewed slots	41
3.7	Full pitch (a) and Fractional pitch (b) windings	43
3.8	Single Layer winding (a) and Double Layer winding (b)	44
3.9	Concentrated winding of single layer (a) and double layer (b)	44
3.10	Lap winding (a) and Wave winding (b)	45
3.11	MMF stator vector when (a) $\omega t = 0^\circ$ and (b) $\omega t = 90^\circ$	46
3.12	Principle of torque production	47
3.13	Equivalent circuit of induction motor	48
3.14	Simplified equivalent circuit of induction motor	49
3.15	Characteristic of induction motor's torque speed	50
3.16	Principle of hysteresis-current PWM	51
3.17	VVVF control characteristic of torque speed	53
3.18	VVVF control operation	53

3.19	Electric machine's active length and the diameter of the air gap	59
3.20	Homogeneous Dirichlet Boundary	62
3.21	Reduction of the surface analysis using Neumann Boundary Condition	63
3.22	Hysteresis Loop	66
3.23	Torque-Speed curves of NEMA Classifications	67
4.1	Development of PM materials	74
4.2	Demagnetization curves of PM materials	76
4.3	Magnetic flux density of a typical ceramic magnet	77
4.4	Operating point of PMs	78
4.5	Simple layout of flux path in electric machine	79
4.6	Simple electromagnetic device with a PM	81
4.7	Ways that magnet can be placed on poles (a) single segment, (b) multiple segments, (c) top of each other	82
4.8	Different shapes of permanent magnets (a) rectangular, (b) radial, (c) breadloaf	83
4.9	(a) Radial and (b) Parallel magnetizations	84
4.10	Magnetic lines and magnetic induction in the air gap for (a) machine with radial magnetization, (b) machine with parallel magnetization	84
4.11	Exploded diagram PM brushless motor exploded diagram	85
4.12	Permanent Magnet Rotor Types	86
4.13	Machine with Inner rotor (left) and Outer rotor (right)	88
4.14	Produced Power of BLAC	90
4.15	Three phase full-bridge inverter topology	91
4.16	Produced Power of BLDC	93
4.17	BLDC trapezoidal waveform	95
4.18	Trapezoidal waveform with hall sensors	96
4.19	Optical encoder position sensor	97
4.20	Definition of torque ripple and cogging torque	101

List of Tables

2.1	Evaluation of electric motor engines	23
2.2	Typical EV Battery Electrical Parameters	29
2.3	Comparison of various Battery Technologies	30
3.1	Possible combinations of concentrated double layer winding	42
3.2	Areas of L / τ	60
3.3	Typical characteristics of all NEMA A class motors	69
3.4	Typical characteristics of all NEMA B class motors	69
3.5	Typical characteristics of all NEMA C class motors	70
3.6	Typical characteristics of all NEMA D class motors	70
3.7	Typical characteristics of all NEMA E class motors	70
4.1	Properties of PM materials	75

Chapter 1

Introduction

1.1 Motivation

We are living in an era that the environmental problems are rising. Vehicles are one of the causes of these problems, providing gas emissions. The substitution of internal combustion engines vehicles with electric vehicles can provide a solution to this problem. The motivation of the present diploma thesis is to make a review of two specific electric motor models. These are the induction motors and the permanent magnet brushless motors, which both are extensively used in the automotive industry for hybrid and electric vehicles. The motor is the basic component of the drive system of a vehicle and is highly responsible for its performance and efficiency. For this reason it is of the utmost importance to understand how each electric motor works precisely, in order to reach the aim of improving them in the near future.

1.2 Thesis Structure

The rest of this thesis is organized as follows:

Chapter 2 provides the background of electric vehicles and their drive systems, introduces the electric motors and power electronics used, and also explains the battery system of an electric vehicle.

Chapter 3 presents an extensive bibliographic investigation of the induction motors. The construction materials, the principle of motor, the inverter and control techniques used, and a preliminary design are presented.

Chapter 4 presents an extensive bibliographic investigation of permanent magnet brushless motors. The construction materials, the placement and the geometry of the magnets and the type of the stator windings are described. A preliminary design is also made.

Finally, Chapter 5 concludes this thesis by discussing our key findings from the study of the electric motors and by presenting some directions for future work.

Chapter 2

Electric Vehicles

2.1 History of Electric Vehicles

Environmental and economic reasons advocate the development and diffusion of a different type of car from the widespread use of internal combustion engines. Emissions of gaseous pollutants from gasoline and diesel vehicles are largely responsible for air pollution and the greenhouse effect leading to global warming. Another disadvantage is dependence on oil, which has important economic and political consequences, increasing as oil reserves are depleted.

The electric car offers an alternative and environmentally friendly way of moving. The high efficiency of the electric drive system and the ability to produce electricity from renewable energy sources offer solutions to the environmental and economic concerns of the aforementioned. The advantages of the electric car make it an environmentally friendly means of transport.

Electric cars have been on the road since the mid-19th century, even before the use of internal combustion engine vehicles [4]. However, some restrictions on their use and difficulties in producing them, coupled with the rapid technological development of internal combustion engines, led to their disappearance from the spotlight in the early 20th century. Interest in the electric car reappeared in the 1960s, when the effects of the widespread use of internal combustion cars were identified. Although electrical vehicles have since been extensively used in public transport, development was not the same for private vehicles.

As a major technological factor that is a long-term brake in the spread of an electric car are the low range of motion, and the difficulty of storing enough energy in accumulators at acceptable cost. Developments in battery technology over recent years are important and research continues to increase the capacity of energy storage media while reducing their weight and cost. Consequently, in recent years there has been an increase in the production and circulation of electric cars. [5]

2.2 Electric Vehicle drive system

The categories in which electric vehicles are distinguished are two, the fully electric vehicles and the hybrid vehicles.

2.2.1 Electric Vehicle

Electric vehicles (EVs) are characterized by the fact that propulsion is provided by one or more electric motors and that the energy source is portable, chemical or electrochemical. Figure 2.1 illustrates the drive system of an electric car powered by a portable power source. Electrical and mechanical equipment that converts the energy of the source into kinetic energy on the wheel is called a propulsion system.

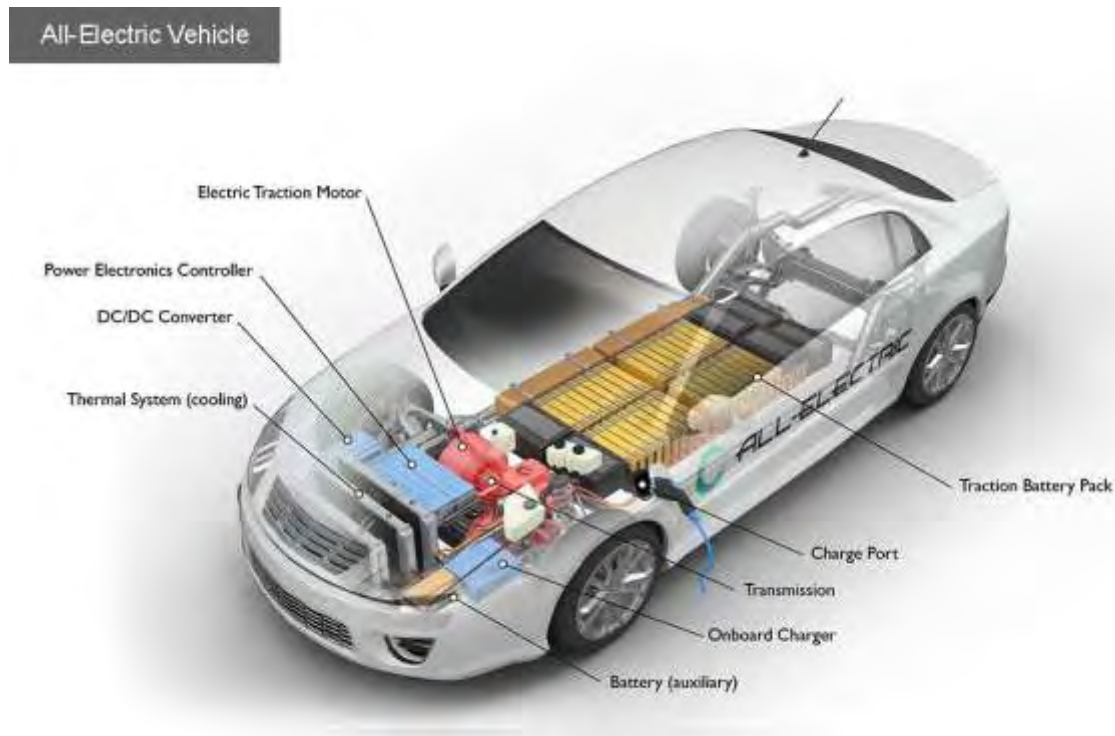


Figure 2.1: Electric vehicle drive system

Charging port or vehicle inlet: It is a connector on the electric vehicle that allows it to be connected to an external source of electricity for charging.

Power electronic converter: A power electronic converter consists of high power, fast acting semiconductor devices, which act as high-speed switches. Different switching states alter the input voltage and current by using capacitive and inductive elements. The result is a voltage output and a current that is different from the input level.

On-board charger: It is an AC-to-DC power electronic converter (often referred to as a rectifier) that takes the incoming AC electricity supplied via the charge port and converts it to DC power for

charging the traction battery. Using the battery management system, it regulates the battery characteristics such as voltage, current, temperature, and state of charge.

Traction battery pack: It is a high voltage battery used to store energy in the electric car and provide power for use by the electric traction motor.

Battery power converter: It is a DC-to-DC power electronic converter that converts the voltage of the traction battery pack to the higher voltage of the DC-bus used for power exchange with the traction motor.

Motor drive: It is a DC-to-AC (often referred to as inverter or the variable frequency drive) or at times a DC-to-DC power electronic converter, used to convert power from the high voltage DC bus to AC (or at times DC) power for the operation of motor. The converter is bidirectional for operating in both driving and regenerative braking mode.

Traction electric motor/generator: It is the main propulsion device in an electric car that converts electrical energy from the traction battery to mechanical energy for rotating the wheels. It also generates electricity by extracting energy from the rotating wheels while braking, and transferring that energy back to the traction battery pack.

Transmission: For an electric car, usually a single gear transmission with differential is used to transfer mechanical power from the traction motor to drive the wheels.

Power electronics controller: This unit controls the flow of electrical power in the various electronic converters in the electric car.

Battery (auxiliary): The auxiliary battery provides electricity in an electric drive vehicle to start the vehicle before engaging the traction battery and is also used to power the vehicle accessories.

The drive subsystems of an electric car are the engine, controller, system drive (converter), power source and transmission. The analytical structure and interaction of the components of such a system is shown in Figure 2.2. The same scheme illustrates the alternatives available for the various subsystems.

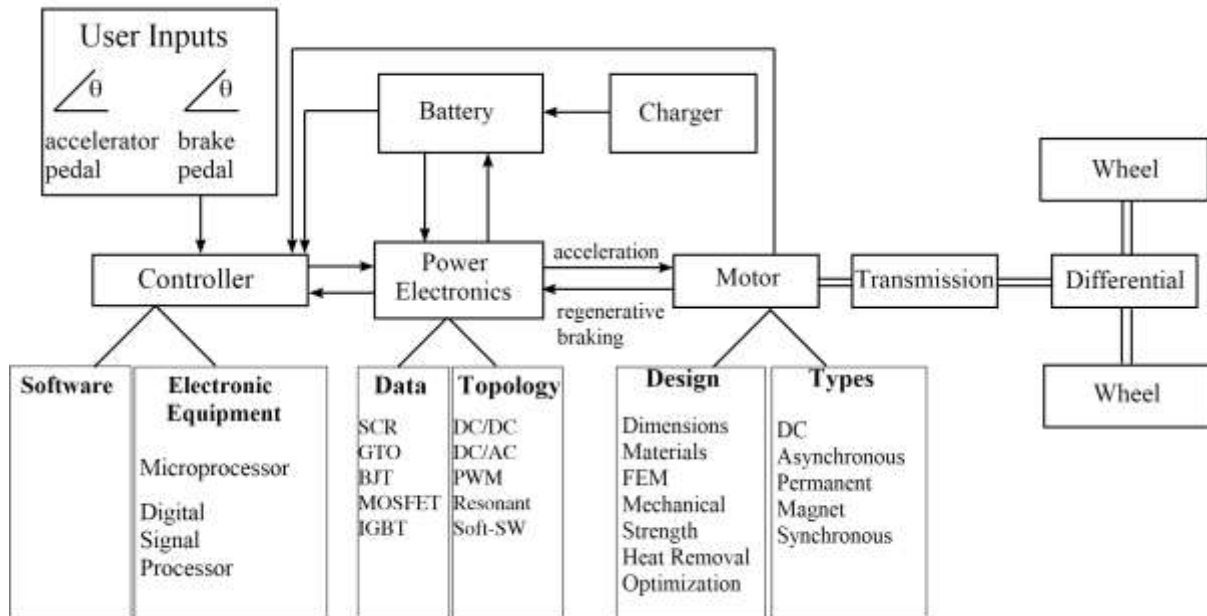


Figure 2.2: Components of the drive system

2.2.2 Hybrid Electric Vehicle

Unlike the electric vehicle, the hybrid electric vehicle (HEV) has at least one power source or a converter that can carry electricity. In the hybrid electric vehicle, propulsion is provided by two or more types of energy sources, inverters or motors, depending on the vehicle's operational status. The hybrid vehicle is a compromise between the benefits of the electric vehicle and the increased range of motion provided by the internal combustion engine. Hybrid vehicles are considered as the short-term solution until the technical and economic issues that prevent the mass production and circulation of the electric vehicles are solved. The main types of hybrid are four: Micro Hybrid, Mild Hybrid or Semi Hybrid, Full Hybrid and Plug-in Hybrid.

Micro-hybrid electric vehicles have the lowest contribution of electric power. In a micro hybrid, the electric motor is used for applications such as stop/start actions of the engine and small scale of regenerative braking. The start/stop functionality can help in turning off the engine automatically at a stop light and hence reduce the fuel consumption. The electric drivetrain, however, cannot be used to supply additional torque to the wheels.

Mild-hybrid electric vehicles have all the functionality of a micro-hybrid. In addition, it has features that allow it to improve the drawbacks of fossil fuel vehicles by improving the efficiency levels. The internal combustion engine (ICE) consumes more fuel and emits more pollutants when coasting,

braking or idling. In those situations the electric motor will assist in order to increase the efficiency levels by helping the engine operation. In a mild hybrid, the electric drive motor can assist the engine when extra power is needed, but it is incapable of propelling the vehicle alone.

A full hybrid electric vehicle has the characteristics that the electric motor provides at least 40% of the maximum range power as additional torque. These types of cars include a large motor and battery bank. This feature gives the opportunity to reduce the size of the combustion. Full hybrid vehicles have three configurations: HEV series, HEV parallel and HEV series-parallel.

- In HEV series configuration electric motor is the only way of delivering power to the wheels (Figure 2.3).

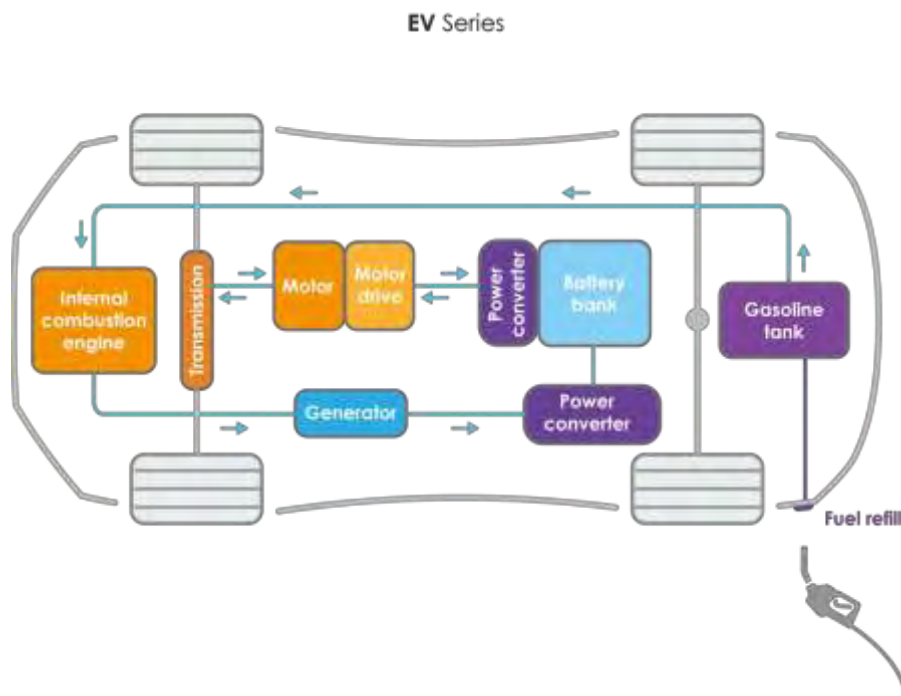


Figure 2.3: HEV series configuration

- In HEV parallel configuration the engine and motor work together to drive the wheels. (Figure 2.4)

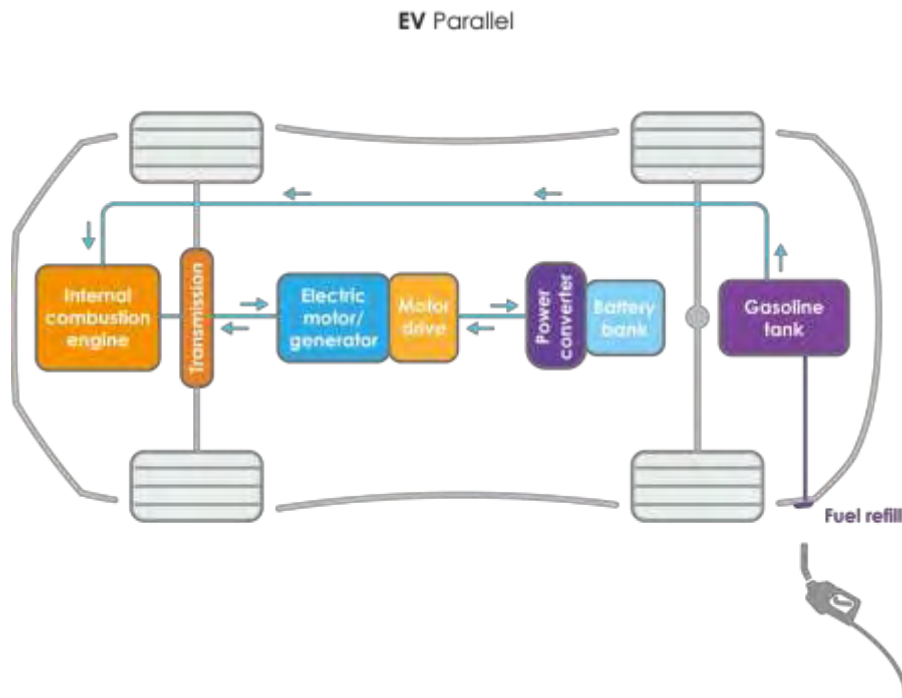


Figure 2.4: HEV parallel configuration

- In HEV series-parallel configuration the engine can directly operate the wheels (parallel arrangement) as well as can be disconnected to give the operation to the electric motors, as in series arrangement. The specific configuration has a clever gearbox, which is called planetary gear set that hooks the gasoline engine, generator and electric motor (Figure 2.5).

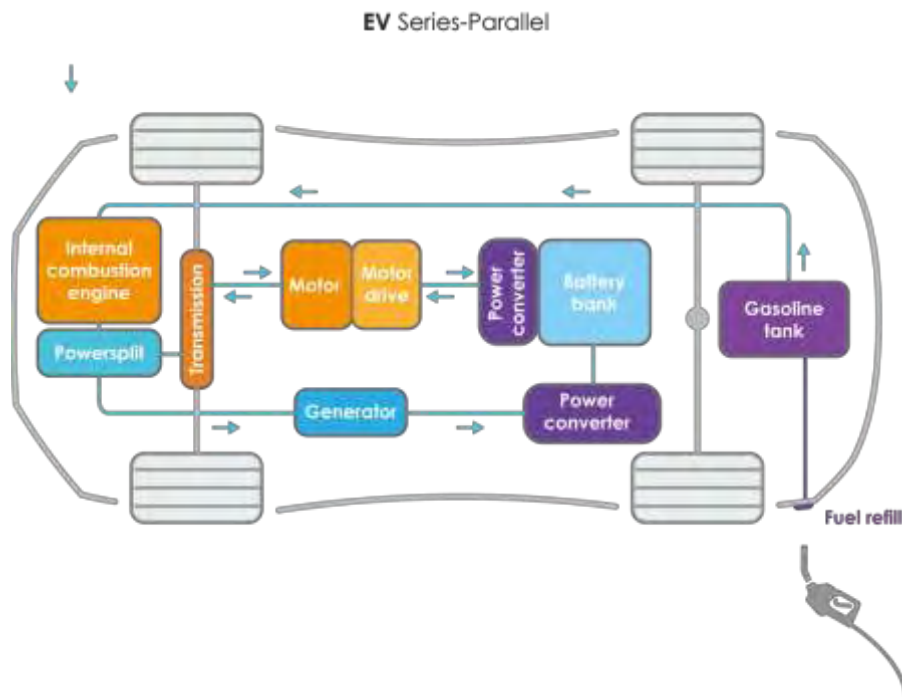


Figure 2.5: HEV series-parallel configuration

- A plug-in hybrid electric vehicle (PHEV) is a hybrid electric vehicle whose battery can be recharged by plugging it into an external source of electric power, as well by its on-board engine and generator. (Figure 2.6)

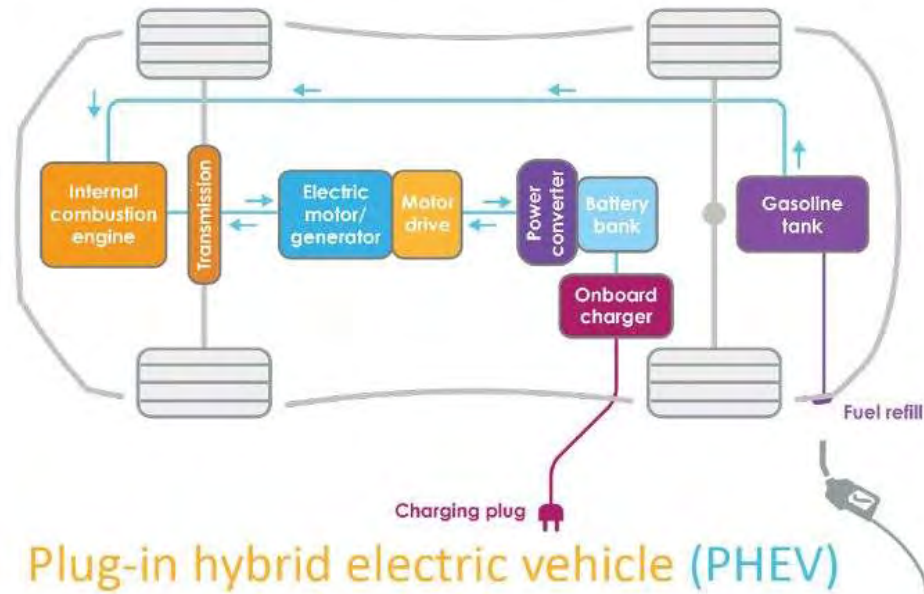


Figure 2.6: PHEV configuration

2.3 Electric Vehicle Motors

2.3.1 Comparative Presentation of Electric Motors

The general specifications to be met by motors used in electric vehicles are high torque at low speeds, a wide range of operating speeds at constant power, high power density, high efficiency, low weight, low cost, reliability and long service life with minimal need for maintenance. Once these conditions have been met, the type of motor that is most suitable for each application is selected. Today, three types of electric motor are used in electric vehicles: Induction motors, Permanent Magnet motors and Synchronous Reluctance motors.

- **Induction Motors**

The AC Induction Motor is a type of motor with wide application to electric vehicles. In this motor the magnetic field is produced by a current that flows through the windings in the housing of stator. If a three phase AC input is used, a rotating magnetic field (RMF) is produced. The magnetic field from the stator induces a voltage and current in the windings of the rotor. Then the rotor produces its own

magnetic field, and this magnetic field makes the rotor turn so as to align itself with the magnetic field from the stator. The rotor follows this rotating magnetic field in the stator, without the need for a commutator with brushes.

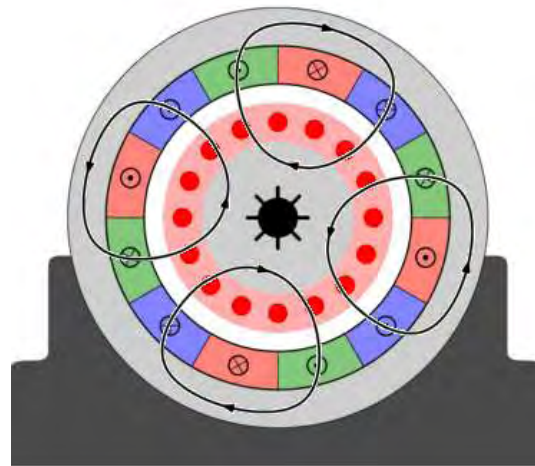


Figure 2.7: Induction Motor

The main causes of their extensive use in automotive market are low cost, easy control and high reliability. Another main reason of using this type of motor today is the ability to subdue in low load conditions in order to achieve a significant high speed, thus significantly improving behavior and performance in conditions constant power control.

- **Permanent Magnet Motors**

The main advantage of Permanent Magnet Motors is the absence of excitation winding, by replacing it with permanent magnets, reducing the relative copper losses while the lack of brushes increases reliability. Permanent magnet motors are an attractive technology for the future solution of electric drive systems due to their extremely high performance, high power density, reduced torque ripple and low acoustic noise. However, their cost remains high due to the cost of permanent magnets and the construction of the complex rotor in order to keep permanent magnets (PMs) at high speeds. In addition, permanent magnet motors are susceptible to high temperatures, as PMs temporarily or permanently degenerate.



Figure 2.8: Permanent Magnet Motor

- **Synchronous Reluctance Motors**

The Synchronous Reluctance motor has neither excitation winding nor permanent magnets on the rotor, taking advantage of only the torque. This type of machine has the advantage of simplicity of construction, low cost and is efficient at higher speeds. Its major drawback, however, is its relatively low power density in terms of weight and volume, limited performance, high torque ripple, heavy acoustic noise and the complex control required by the drive system. Synchronous Reluctance is a special version of the Switched Reluctance, where the magnitude of the magnetic resistor is changed in a smoother sinusoidal way. This greatly improves the control strategy and reduces torque and acoustic noise but it further reduces the power density of this type of engine.

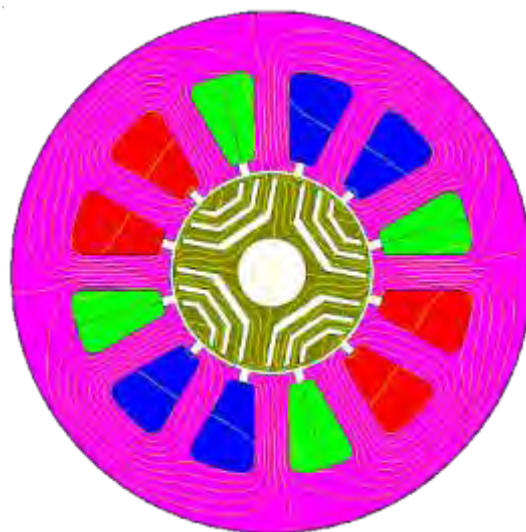


Figure 2.9: Synchronous Reluctance Motor

In order to assess the suitability of the main categories presented above in electric vehicle propulsion applications, a scoring system is used here. Six key motor characteristics are evaluated and the scale ranges from one to five. As shown in Table 2.1, induction motors are offered for use in such vehicles. Also, permanent magnet motors are another solution, which becomes more economically viable as the cost of permanent magnets is reduced. An important breakthrough that has led to a reduction in the cost of permanent magnets is that of the Neodymium-Iron-Boron alloy in 1982.

	Induction Motor	Permanent Magnet Motor	Synchronous Reluctance Motor
Power Density	3.5	5	3.5
Performance	3.5	5	3.5
Control	4	4	3
Reliability	5	4	5
Technological Maturity	5	4	4
Cost	5	3	4
Total	26	25	23

Table 2.1: Evaluation of electric motor engines

2.4 POWER ELECTRONICS

The power between the various power sources and power consumers in an electric vehicle is converted by using power electronic converters. A power electronic converter is an electronic device made of high power semiconductor switches that uses different switching states to change the magnitude and waveform of the voltage and current between the input and output.

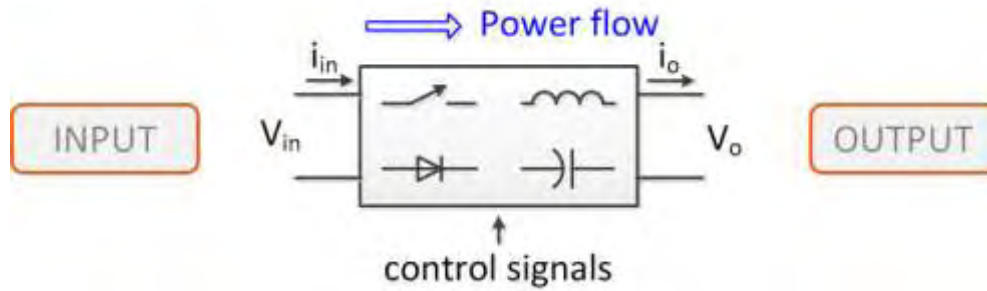


Figure 2.10: Power electronic converter principle

Power semiconductor devices are widely used in automotive power electronic systems, and often dictate the efficiency, cost, and size of these systems. Commercially available power semiconductor devices can be categorized into several basic types such as diodes, thyristors, bipolar junction transistors (BJT), power metal oxide semiconductor field effect transistors (MOSFET), insulated gate bipolar transistors (IGBT), and gate turn-off thyristors (GTO). In addition, there are power integrated circuits (ICs) and smart power devices that monolithically integrate power switching devices with logic/analog control, diagnostic, and protective functions. Emerging device technology is based on silicon carbide (SiC) power devices. SiC is generally considered the most promising semiconductor material to replace silicon in future power electronic systems. Therefore, with the development of power electronics, engineers are given the opportunity to create advanced control devices and develop complex algorithms. By using the power electronic converters, it is possible to supply the motors with variable amplitudes and frequencies, which makes it possible to fully control the engine. At the same time, there are constantly evolving various control techniques that allow for proper drive of the power converter through electronic systems. Now every modern high performance electric drive system is accompanied by the appropriate power converter, the right hardware and control software.

There are four types of power converters:

1. DC-DC converter
2. DC-AC converter (or) inverter
3. AC-DC converter (or) rectifier
4. AC-AC converters

Further, power converters can be bi-directional or uni-directional, isolated or non-isolated. The three basic ways to classify a power converter are shown in the table below:

Type				
AC or DC	AC-DC	DC-AC	DC-DC	AC-AC
Magnetic Isolation	Isolated		Non-isolated	
Bidirectional power flow	Bidirectional		Unidirectional	

2.5 Batteries and Energy Storage Systems

The Energy Storage Systems of electric vehicles are the main drawback in their development and consolidation as a key factor in transport in the industry today. Two major technological factors that affect the progress of electric vehicles are the low range of motion and the difficulty of storing enough energy in accumulators at acceptable cost. Although the electric vehicle has a significant lead in utilizing the available energy reserve due to its overall high degree of efficiency, liquid fuels offer much greater range, at today's technological level.

Even today, the cost of the battery is significantly higher than that of the motor and therefore the utilization rate of the stored energy becomes the first priority in the design and implementation of the entire drive system [2]. However, battery technology developments in recent years are significant and research continues to increase the capacity of energy storage media while reducing their weight and cost. The gradual improvement of energy density in storage units is expected to have a significant impact on the current design strategies of the other power system, which is currently geared towards optimal energy utilization, thus hampering performance for performance.

2.5.1 Fundamental Characteristics of Batteries

The battery converts chemical energy into electrical energy and vice-versa respectively at the time of charging and discharging. The electrochemical battery is a combination of independent cells which

possess all the electrochemical properties. Each cell is capable to store or deliver a significant amount of energy individually or in combination based on their connections. High energy density, high power density, modularity, flexibility and affordability are the factors that guide the battery technology on the roadmap of vehicle electrification [3]. In electric vehicles, battery stores major onboard energy and contain high energy and power density to meet complete driving cycles of vehicle operation.

An electric vehicle requires increased power density from the battery system in order to be able to get power directly to allow acceleration (propulsion) or deceleration (regenerative braking). The motion of a vehicle is characterized by audible transients which require development of significant force ($> 40\text{kW}$), the magnitude of which is at least 5-10 times bigger than that required in a household medium at full load (8kVA). Normally even the braking system of a conventional vehicle (brakes) is about four times stronger than that of propulsion (petrol). For example, a car with 100 hp engine has braking capacity of about 400 horsepower, indicating for the respective electric vehicles that the regenerative braking is particularly demanding in terms of energy storage capacity back to the battery system. Battery's power density is directly related to its internal resistance and hence allows, besides a rapid discharge (propulsion), a rapid charging, exploiting in this way the dynamic effects during the regenerative braking, without the need of wasteful energy, which because of the magnitude of power, cannot be returned to the storage system and is discharged as heat.

The second characteristic of the electric battery system is the energy density. Energy density determines the volume and weight of the battery, which is necessary to store a certain amount of energy. When designing battery cells, there are limitations on how to reconcile power density and energy density offered by each technology. At today's technological level, a fairly good compromise between these features exists, allowing for the development of electric vehicles as viable competing products. However, the cost is not a negligible parameter for the viability of the electric vehicle, where even on a large-scale production scenario, it is extremely difficult for today's car manufacturers to produce an electric vehicle competing with the respective thermal, only because of high battery costs.



Figure 2.11: Battery pack of a Tesla Model S electric vehicle.

The main disadvantage of the battery as a vehicle energy storage compared to the fuel cells is the inability to independently dimension the energy density and power density as the energy-carrying device itself is also responsible for the power output. For example, an 80kg battery system has a power capacity of 30kW and a power storage capacity of 10kWh. If it is desired to reduce the energy to 5kWh, because it was decided in the preliminary design, this would entail a mandatory reduction of the power capacity by half to 15kW. Exactly the same applies with the dimension of the power, which will have an impact on the stored energy. Instead, the fuel cells are devices that are dimensioned to the desired power, while the energy dimensioning is through the fuel bottle, giving flexibility to design and cost. However, the fuel cells have other, far more serious disadvantages compared to batteries, which make them less preferable for electric propulsion today.

2.5.2 Security of EVs and System of Batteries

The issue of safety offered by the presence of a battery in the electric vehicle is of great importance. The security issue focuses on the development of techniques and systems to avoid the risk of electric shock due to high voltage, explosion, fire and high temperature risks due to the large amount of energy and poor road behavior of the vehicle due to the heavy weight of the battery system. The placement of the battery system is preferably made in the lowermost part of the vehicle, as shown in Figure 10. This ensures acceptable vehicle road behavior by displacing the center of gravity of the vehicle as low as possible.

The existence of high voltage, which in a battery system can take values particularly dangerous to human life, requires special care when designing. Vehicle battery systems typically have isolation switches, both between the battery and the inverter, as well as between battery cell groups, so that the voltage drops immediately, interrupting the connections between the groups in the event of an accident or need [2]. Typically, the grouping relays are also supported by lateral acceleration sensors, which predict the irregular behavior of the vehicle and interrupt before the vehicle crashes. The battery system terminals are not connected to any part of the vehicle, as was traditionally done on conventional vehicles. Thus, the entire drive system has no common trend reference point with the vehicle frame.



Figure 2.12: Complete Storage System of Batteries of General Motor electric vehicle

Particularly serious is the issue of thermal safety due to the large amount of energy stored in the battery system. An amount of energy of 10-20 kWh is able to develop high temperatures and cause melting of mechanical parts and metals surrounding it, even the floor of the vehicle, with immediate danger to passengers and nearby attendees. Vehicle battery components are equipped with a particularly durable housing so that in the event of an accident, it is difficult to short-circuit due to conduction of the elements between them in such a way that a relay does not interfere. In addition, separating the data into groups allows, apart from partitioning and isolation in smaller energy groups, even if a group is damaged due to a short circuit, the possibility of chain catastrophe is prevented. Typically, battery grouping in tension is combined with energy grouping, leading to space-conscious and galvanic isolation groups within the unit's enclosure.

2.5.3 Technology of Batteries

The power and energy requirements for different types of EV's in comparison with HEV and PHEV are listed in the Table 2.2, together with common voltage ratings.

EV type	Power (kW)	Energy (kWh)	Voltage (V)
HEV	20 - 50	1 - 3	200 - 350
PHEV	>40	2 - 15	200 - 500
BEV	>80	25 - 100	200 - 1000

Table 1.2: Typical EV Battery Electrical Parameters

There are plenty of materials and electrolytes that can be combined to form a battery. However, only a relatively small number of such combinations have developed into commercially available rechargeable batteries. These include Lead Acid, Nickel based (NiMH, NiCad), high temperature Sodium-Nickel-Chloride (NaNiCl or Zebra), Lithium-ion (Li-ion) and Lithium-polymer (Li-poly). There are also more recent developments with batteries that can be recharged mechanically. In this category is the Aluminium air (Al-air) and Zinc-air (ZN-air).

The Table 2.3 shows a comparison of different battery technologies [3]. Briefly reference is made to two types of battery technologies, lithium-ion batteries and metal-air batteries. The first technology is the most current available technology, while the second is a promising solution for the years to come.

Advantages ON OVER		Lithium Based		Nickel Based		Lead Acid
		Ion	Polymer	Nickel Metal Hydride Ni-MH	Nickel Metal Cadmium Ni-CD	
Lithium based	Ion		<ul style="list-style-type: none"> Gravimetric Energy density Design characteristics Safety Price 	<ul style="list-style-type: none"> Price Safety Discharge rate Recyclability 	<ul style="list-style-type: none"> Operating temperature range Higher cyclability Price Safety Recyclability 	<ul style="list-style-type: none"> Higher cyclability Price Safety Recyclability
	Polymer	<ul style="list-style-type: none"> Operating temperature range Higher cyclability 		<ul style="list-style-type: none"> Volumetric energy density Higher cyclability Price 	<ul style="list-style-type: none"> Operating temperature range Higher cyclability Price 	<ul style="list-style-type: none"> Higher cyclability Price
Nickel based	Nickel Metal Hydride NiMH	<ul style="list-style-type: none"> Gravimetric energy density Volumetric energy density Operating temperature range Higher cyclability Voltage output Self discharge rate 	<ul style="list-style-type: none"> Gravimetric energy density Volumetric energy density Operating temperature range Self discharge rate Design characteristics 		<ul style="list-style-type: none"> Operating temperature range Higher cyclability Self discharge rate Price 	<ul style="list-style-type: none"> Higher cyclability Voltage output Price
	Nickel Cadmium NiCd	<ul style="list-style-type: none"> Gravimetric energy density Volumetric energy density Voltage output Self discharge rate 	<ul style="list-style-type: none"> Gravimetric energy density Volumetric energy density Self discharge rate Design characteristics 	<ul style="list-style-type: none"> Gravimetric energy density Volumetric energy density 		<ul style="list-style-type: none"> Higher cyclability Voltage output Price
	Lead Acid	<ul style="list-style-type: none"> Gravimetric energy density Volumetric energy density Voltage output Self discharge rate 	<ul style="list-style-type: none"> Gravimetric energy density Volumetric energy density Self discharge rate Design characteristics 	<ul style="list-style-type: none"> Gravimetric energy density Volumetric energy density Self discharge rate 	<ul style="list-style-type: none"> Gravimetric energy density Volumetric energy density Operating temperature range Self discharge rate Reliability 	
	Absolute Advantages	<ul style="list-style-type: none"> Gravimetric energy density Volumetric energy density Self discharge rate Voltage output 	<ul style="list-style-type: none"> Gravimetric energy density Volumetric energy density Self discharge rate Voltage output Design characteristics 	<ul style="list-style-type: none"> Volumetric energy density 	<ul style="list-style-type: none"> Operating temperature range Price 	<ul style="list-style-type: none"> Higher cyclability Price

Table 2.3: Comparison of various Battery Technologies

- Lithium Ion (Li-Ion) Batteries

Lithium-ion batteries are more chemically stable than lithium metal batteries. Their chemical stability guarantees greater safety, as well as increased lifecycle. Due to the above features, lithium-ion batteries are preferred for use in electric cars, despite the slightly lower energy density compared to lithium-metal batteries. Their most important advantages are:

- High energy density
- Low self-discharge
- Long life
- No maintenance required
- Wide range of operating temperatures
- High rate capabilities
- Ability to be manufactured in very small sizes and very thin forms

Certainly they also have weak points, such as:

- Relatively high initial cost
- Require a surveillance system to avoid overloading or overexploitation

Some of the above disadvantages are being treated with ever greater success. The cost is constantly decreasing. Some lithium-ion batteries, especially those with polymers, can operate with simplified protection circuits. Also, their output power has increased significantly thanks to the use of new descent materials.

- Metal Air Batteries

Aluminium-air (Al-air) and zinc-air (Zn-air) batteries both use oxygen absorbed from the atmosphere on discharge and expel oxygen when being charged. The energy density of these batteries is high but, lower power densities mean that applications are limited. Al-air batteries consume the aluminum electrode, and must be removed and replaced or reprocessed. Some applications have been tested where fleets of EV delivery vehicles are running with Zn-air batteries, where removable zinc cassettes can be replaced when discharged for recharged units. The low specific power of metal air batteries may see these battery types restricted to long distance delivery vehicles, but the advantages of regenerative braking may be sacrificed.

2.5.4 Battery Management System (BMS)

Batteries for electric vehicles consist of many interconnected cells in combination forming a battery pack. Individual battery cells show a reduction in capacity with increasing charge and discharge cycles, as well as variations in temperature. When cells are connected in a series or parallel configuration as in a battery pack, management and control of the charge and discharge conditions becomes crucial to extend the lifetime and limit ageing effects of individual cells. A battery management system (BMS) is used to monitor, control and balance the pack. The main functions of a BMS are outlined in the Figure 2.13. Without balancing the battery pack, the battery is not only risking unnecessary damage, it is also operating sub-optimally. Because the worst cell is limiting the performance of all cells in the battery pack, it is very important to prevent big differences in cell's state of charge.

The cost and complexity of a BMS depends on the functionality and intelligence built into the management system. State-of-charge (SOC) estimation is an important parameter to measure accurately, especially if EV's are integrated with a smart electrical grid.

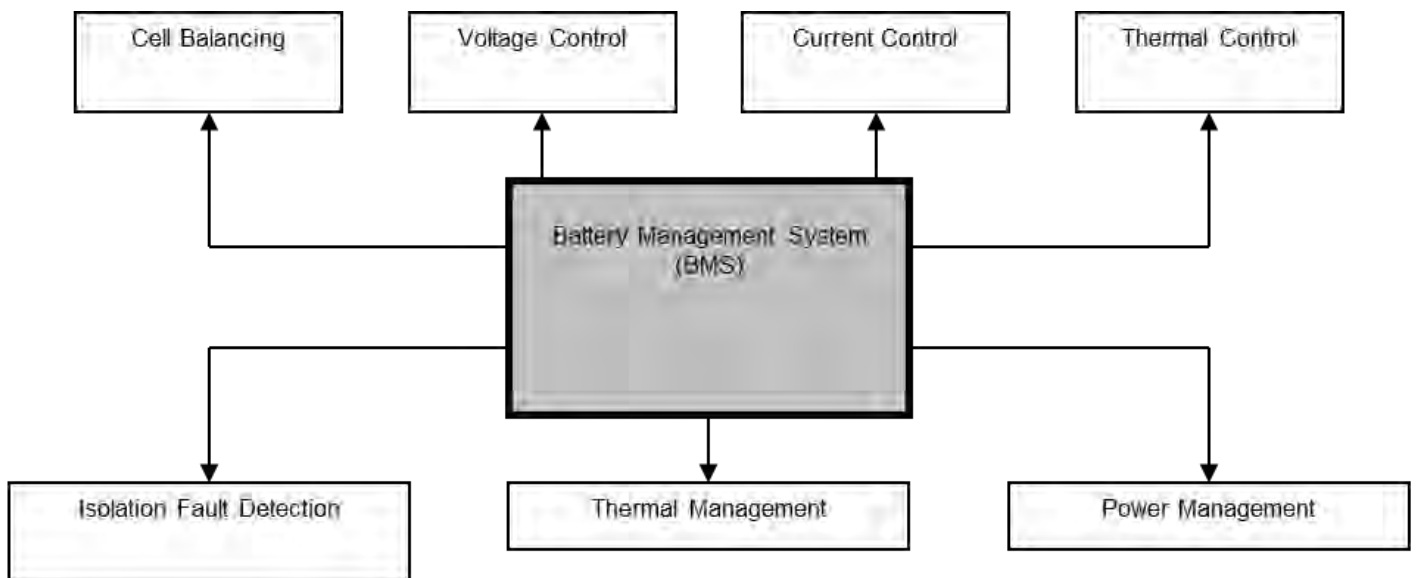


Figure 2.13: Battery Management System (BMS)

Because the performance of battery cells varies with temperature, it is therefore crucial to include a thermal management system in the battery pack. This ensures all cells are both electrically and thermally balanced and the lifetime will be extended. Thermal management systems can either use air or liquid as the transfer medium. For integrating into the vehicle, the power consumption must be low and it must not add much additional mass. The thermal management system can realize its performance requirements using either passive or active means. A passive system using only the ambient environment may provide sufficient thermal control for some battery packs whereas active control may be required for others.

The BMS has the possibility to monitor and control (directly or indirectly) several different parameters of the battery:

1. Voltage
2. Current
3. State of charge
4. Temperature
5. State of health

First of all, the **voltage** of the total battery pack and of the individual cells is monitored by the BMS. The BMS can keep track of the difference between the minimum and the maximum cell voltages, and estimate if there is a dangerous imbalance in the battery pack. The charging and discharging **current** of the battery pack is essential to control, as too high current can overheat a battery and lead to a failure. Further, improper control of the charging and discharging current can lead to overvoltage and under voltage of the battery, respectively that can harm the battery on the long run.

The **state of charge (SOC)** function is extremely important to keep track on, because many batteries must not be discharged below a certain percentage. This is because, if the depth of the discharge becomes too high, some batteries can start to break down or lose their capacity. The state of charge can be determined from the measured values of the voltages and currents.

Another function is the **temperature** of the battery pack and the individual cells. Temperature is directly related to the battery lifetime, as high temperatures can degrade the battery faster. The individual cell temperature is important to know as well, to see if there are local hot spots, indicating a possible failure. Using the BMS together with the battery thermal management system can cool the

battery and keep it within a nominal range. When there is a coolant available, the temperature of the intake and output coolant temperature is an important indicator of the temperature of the battery pack.

The **state of health** is a measurement to estimate the overall condition of the battery with respect to lifetime. Battery cell balancing is key feature of the BMS to help increase battery lifetime. Naturally after a while, the different cells in a battery pack will start to show differences in the state of charge and thus show localized under or overcharging. This can have multiple causes. For example: manufacturing inconsistencies, different charging/discharging currents, heat exposure and more. This is detrimental to the lifetime of the battery pack, because most cells in the battery pack are connected in series (adding voltages). This means that if 1 battery cell breaks down, the whole battery pack will seem to be broken (zero current). The BMS can perform balancing in a passive or active way. In case of passive cell balancing, passive elements such as resistors are used. This is simple but inefficient as it leads to power losses in the resistors. On the other hand, in case of active balancing, DC-DC power electronic converters are used to equalize the cells and reduce the differences between the operational state of individual cells.

Chapter 3

Induction Motors

Induction motor drives offer several benefits for electric propulsion. They are currently the most developed technology in a variety of motor drives without a commutator. There are two types of induction motors (IMs): the squirrel cage and the wound. The wound-rotor induction motor is not as attractive as the squirrel cage, particularly for electric propulsion in electric vehicles (EVs), due to its high costs, maintenance requirements and lack of robustness. The squirrel cage induction motor is therefore broadly referred to as the induction motor for EV propulsion. The induction motor drives have the advantages of robustness and low cost, adding to the existing benefits of motor drives without a commutator. These benefits can mostly compensate for their major drawback of complex control and facilitate the acceptance of this technology by EVs.

Squirrel-cage induction motors are simple in structure, reliable and robust. They have low maintenance requirements and are available at highly competitive prices. Their costs are significantly lower than those of commutator machines, and their efficiency is similar. All these characteristics make their use in industrial drives applications attractive.

The three-phase armature winding of the stator creates a rotating magnetic flux that rotates at synchronous speed. The synchronous speed is related to the pole number of the motor and the supplied frequency. The rotating magnetic flux created by stator windings, crosses the rotor's armature winding and induces an electromagnetic field (EMF) in the rotor winding, which leads to the existence of a current. As a result, rotor's currents create a second magnetic flux, which interacts with stator's magnetic flux, producing a torque to accelerate the motor. The voltage of the rotor decreases in magnitude and frequency as the rotor accelerates, until the desired speed is achieved. Synchronous speed is always slightly higher than the rotor speed by the "slip" frequency, which is usually 3%. The only way to ensure constant excitation of the motor, and to maximize torque production up to the base speed, is to ensure that the ratio of stator voltage to frequency is almost constant.

3.1 Structure of Induction Motors

As mentioned before, the squirrel-cage induction motor is the most used type of induction motors. The structure of the motor is shown in Figure 3.1 [7]. It consists of a stator with three phase armature windings, a rotor with cage bars that are short circuited by two end rings, which can also be molded

with fan blades to provide better cooling of the motor during the rotation, two end bearings to support the rotor, and a motor frame with two end bells to house the motor.

In Figure 3.2 is shown a three phase two pole induction motor, in which the stator has three phase armature windings connected as A-X, B-Y, and C-Z, and the rotor is installed with squirrel-cage bars (the so-called cage bars). The current of the stator windings produce a sinusoidal distribution of air gap flux density. The cage bars are short circuited via the front and rear end rings.

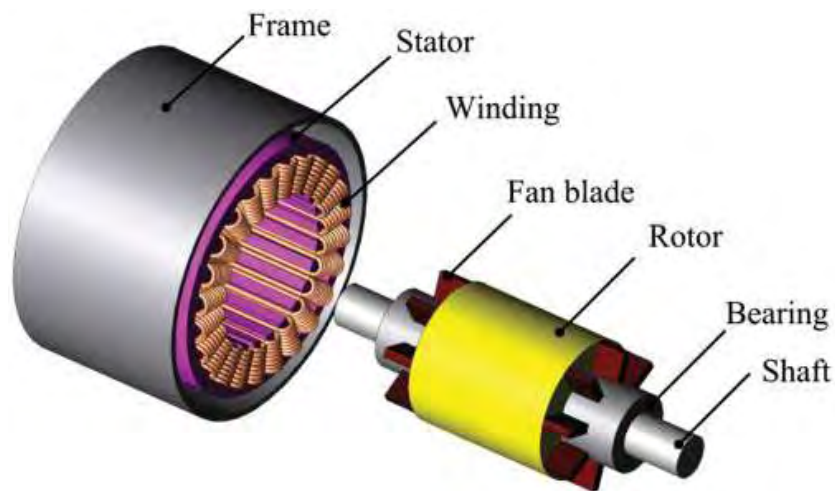


Figure 3.1: Structure diagram of Induction Motor

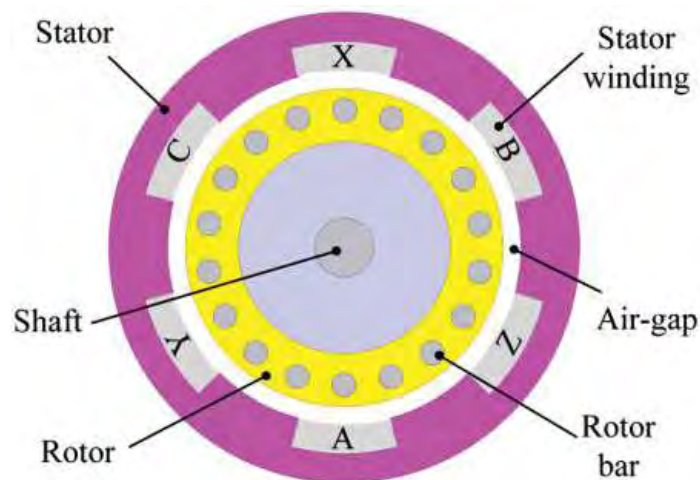


Figure 3.2: Induction motor topology

Below in Figure 3.3 is shown an infrequent three phase sixteen pole induction motor with outer rotor. Here the principle remains the same as the common inner rotor induction motor topology. The outer rotor topology design resembles the “pancake” shape and has large radial diameter and short axial length, which offer the ability to have many numbers of poles, and therefore direct in-wheel drive as an option.

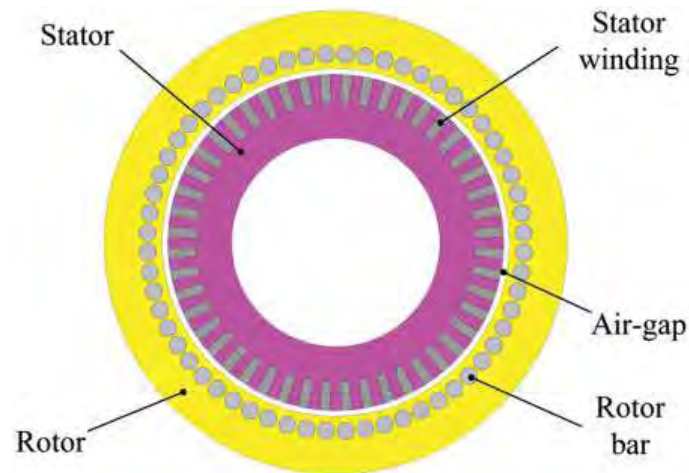


Figure 3.3: Outer-rotor Induction motor topology

3.1.1 Stator

The stator is made of thin sheets of aluminum or iron which are joined together to form a hollow cylinder, the stator core, with slots as shown in the Figure 3.4. The existence of slots in stator provides a structurally small magnetic air gap, resulting to increased permeability coefficient and magnetic flux density of the air gap. This implies a higher output torque and increased efficiency. Also, the large contact area between the windings and the stator provides good heat dissipation from windings to the environment.

The windings are normally placed on the evenly distributed stator channels of the stator ferromagnetic material. To form a complete winding, similar coils are placed in opposite slots and then connected together in groups. Coil groups of three-phase motors are connected to a star or delta. The windings may be single or double layer. In the double layer windings each slot contains two coil sides, one at the top and one at the bottom. Each coil has one side at the top and the other at the bottom of the slot. Depending on the winding and power supply, the machine may have any number of magnetic poles.

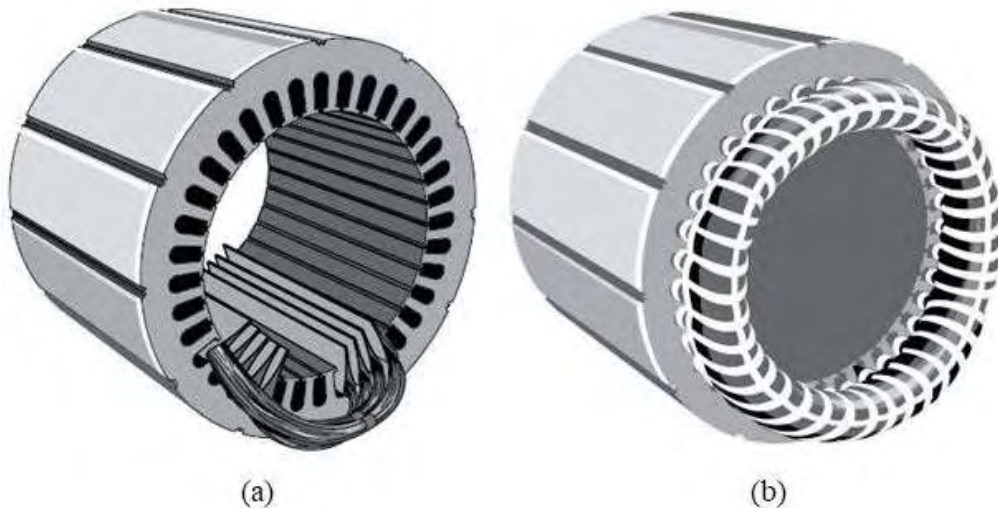


Figure 3.4: Stator with (a) partially completed winding and (b) completed winding

The number of stator slots should be carefully chosen at the design phase, as this number affects the cost, weight and operating characteristics of the motor. Although there are no rules to select the number of stator slots, taking into account the advantages and disadvantages of selecting higher slots, the number of slots must be selected. Less slots offers less cost and less space lost due to insulation and slot opening. On the other hand, more slots offers smaller leakage inductance and larger breakdown torque, small magneto-motive force (MMF) harmonics and better cooling. In general, the combinations of poles and slots to which the two types below apply, present asymmetrical magnetic attraction and should be avoided:

$$p = Q_s \pm 1$$

$$Q_s = 9 + 6k$$

- **Asymmetrical Magnetic Attraction**

If the magnetic forces are not distributed correctly on the air gap, their sum leads to a one-sided magnetic force, which rotates with each turn of the motor in the air gap [5]. This is a phenomenon that causes intense noise and vibration on the shaft. This phenomenon can be observed visually in the Figure 3.5 (a) and (b), for a 68-pole and 69-slot machine. While in Figure 3.5 (c) and (d) are depicted two machines that do not exhibit asymmetrical magnetic attraction.

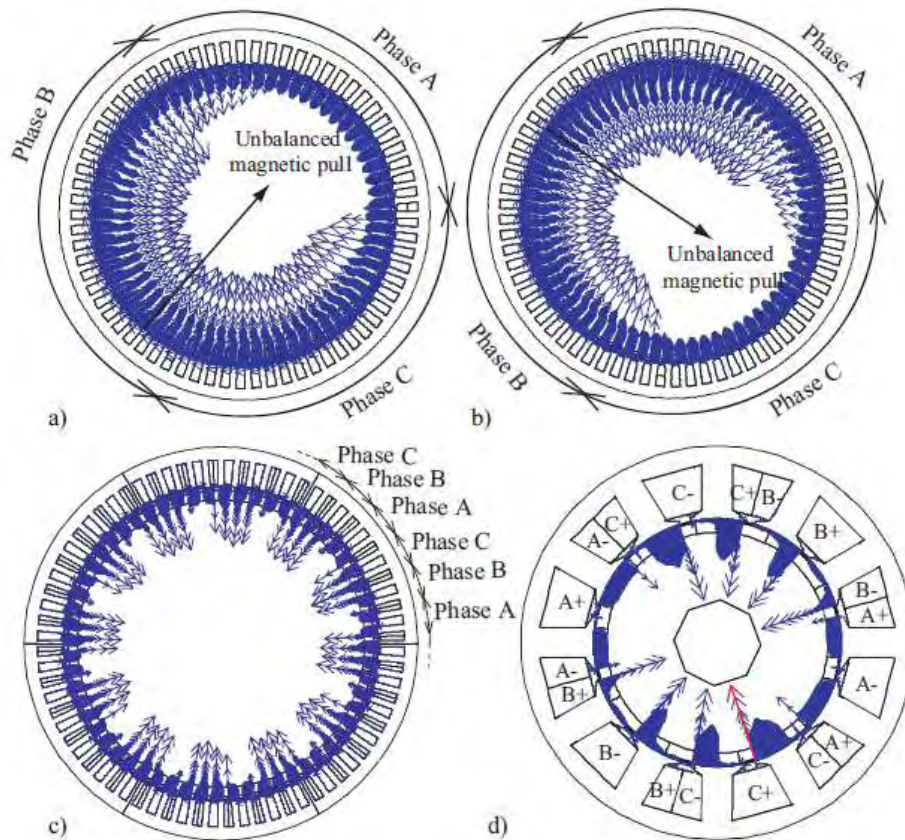


Figure 3.5: In (a) and (b) is observed a machine with 68 poles and 69 slots in two different times, (c) a machine with 60 poles and 72 slots and (d) a machine with 10 poles and 12 slots

3.1.2 Rotor

There are two main types of rotors that are used in induction motors, the squirrel cage rotor and the wound rotor. However, only the squirrel cage rotor induction motor is used in the EVs industry. As a result, wound rotor will not be discussed.

The rotor consists of numerous thin laminations of steel along the periphery with evenly spaced bars made of aluminum or copper. These bars are mechanically and electrically connected at the ends through the use of rings in the squirrel cage rotor. A vast majority of induction motors have squirrel cage rotor due to its rugged and simple construction. The rotor consists of a cylindrical laminated core with axially placed parallel slots for carrying the conductors. Every slot has a bar made of an aluminum, alloy, or copper. These rotor bars are permanently short-circuited with end rings at both ends, as shown in Figure 3.6. This total assembly looks like a squirrel cage that gives its name to the rotor.

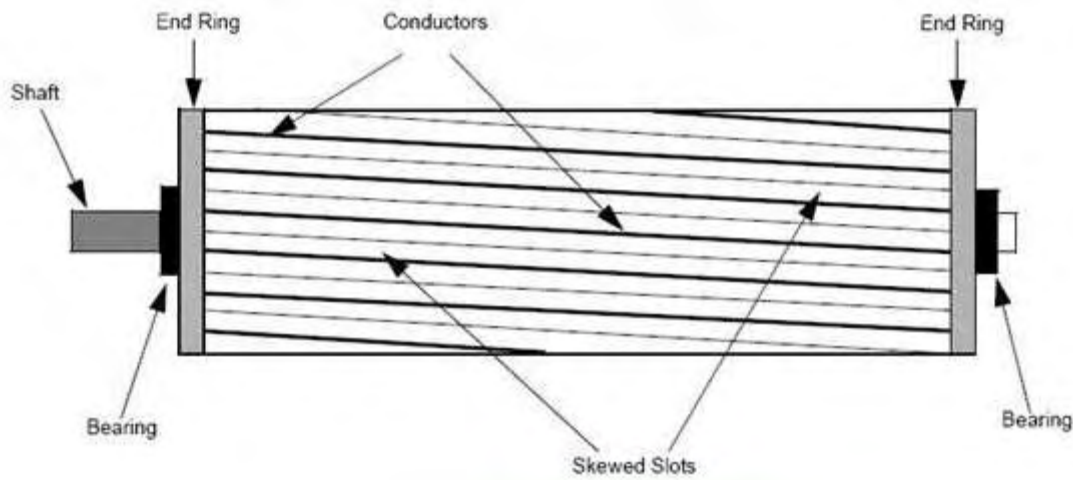


Figure 3.6: Squirrel cage rotor with skewed slots

The slots of the rotor have a skew and are not precisely parallel to the shaft, for two main reasons. The first reason is the reduction of magnetic hum and the decrease of slot harmonics that keep the motor running quietly. The second reason is to reduce the rotor's locking tendency. Due to direct magnetic attraction, the rotor teeth tend to remain locked under the stator teeth. This occurs when the number of stator teeth is equal to the number of rotor teeth. The rotor is mounted on the shaft with bearings on each end. As shown in Figure 3.6, usually one end of the shaft is longer than the other for driving the load. For mounting speed or position sensing devices, some motors may have an accessory shaft on the non-driving end. There is an air gap between the stator and the rotor through which the energy is transferred by induction from the stator to the rotor. The produced torque forces the rotor and then the load with it to rotate. Regardless of the rotor type, the principle of rotation remains the same.

3.1.3 Windings

The choice of the type of winding of the motor is aimed at the better spatial distribution of the rotating magnetic field. Stator windings can be divided into two main categories: concentrated winding and distributed winding, which distributed in turn is divided in lap windings and wave windings. Lap windings are commonly found in low pole motors, multi-speed motors or heat station generators and the wave windings can be found in low-speed engines or hydroelectric power generators.

- **Distributed Winding**

Distributed winding is the most established and widely used option. It offers sinusoidal distribution of magnetic flux in the air gap. The coils of each winding are appropriately distributed in the slots to form full or fractional pitch coils. The more coil sides per pole and phase, the better we approach the sinusoidal waveform. Distributed winding is used in cylindrical machines, is operated on high speed machines and has low number of poles.

- **Concentrated Winding**

In concentrated winding all the winding turns are wound together in series to form one multi coil. Concentrated winding may not have such good characteristic sinusoidal distribution, but it is a kind of winding that is of great interest in recent years. This is due to its advantages, some of which are high performance, short winding edges, high load factor, high power, low cogging torque, high error tolerance, flux weakening and easy manufacturing, resulting in lower production costs [9].

$Q_s \backslash p$	4	6	8	10	12	14	16	18	20	22	24	26	28	30	32	34	36	38	40
6	0.866		0.866	0.5		0.5	0.866		0.866	0.5		0.5	0.866		0.866	0.5		0.5	0.866
9	0.617	0.866	0.945	0.945	0.866	0.617	0.328		0.328	0.617	0.866	0.945	0.945	0.866	0.617	0.328		0.328	0.617
12	$q=1$		0.866	0.933		0.933	0.866								0.866	0.933		0.933	0.866
15			0.621	0.866		0.951	0.951		0.866	0.621								0.621	0.866
18		$q=1$		0.647	0.866	0.902	0.945		0.945	0.902	0.866	0.647							
21						0.866	0.89		0.953	0.953		0.89	0.866						
24			$q=1$			0.76	0.866		0.933	0.95		0.95	0.933		0.866	0.76			
27								0.866	0.877	0.915	0.945	0.954	0.954	0.945	0.915	0.877	0.866		
30				$q=1$					0.866	0.874		0.936	0.951		0.951	0.936		0.874	0.866
33									0.866			0.903	0.928		0.954	0.954		0.928	0.903
36					$q=1$						0.866	0.867	0.902	0.933	0.945	0.953		0.953	0.945
39												0.866	0.863		0.918	0.936		0.954	0.954
42						$q=1$							0.866		0.89	0.913		0.945	0.953
45														0.866	0.859	0.886		0.927	0.945
48							$q=1$								0.866	0.857		0.905	0.933
51																0.866		0.88	0.901
54								$q=1$									0.866	0.854	0.877
57																		0.866	0.852
60									$q=1$										0.866

 	$q=1/2, 1/4$	 	$q=3/8, 3/10$	 	$Q_s=21+6k, p=Q_s \pm 1, k = 0, 1, 2 \dots$
 	$q=3/7, 3/11$	 	$q=5/14, 5/16$	 	$Q_s=24+6k, p=Q_s \pm 2, k = 0, 1, 2 \dots$
 	$q=2/5, 2/7$	 	not appropriate	 	$k_{w1} < 0.866$

Table 3.1: Possible combinations of concentrated double layer winding

If the poles and the slots of a machine are known, a quick way to find out if its winding is concentrated is to look at the number of slots per pole and phase q . This figure is given by the basic relationship:

$$q = \frac{Q}{mP} \tag{3.1}$$

Where, m is the number of phases (usually $m = 3$). If $q < 1$, then the type of winding is concentrated.

- **Fractional Slot Winding**

Windings in which the number of slots per pole and phase is not integer but fractional are called fractional pitch windings. In practice, this means that the coils are positioned in such a way that they are closer in length than the full-pitch windings. For example, a $5/6$ pitch coil covers five-sixths of the distance between two successive poles of the machine. In Figure 3.7, the same topology is represented, initially with full pitch winding and then with fractional pitch winding.

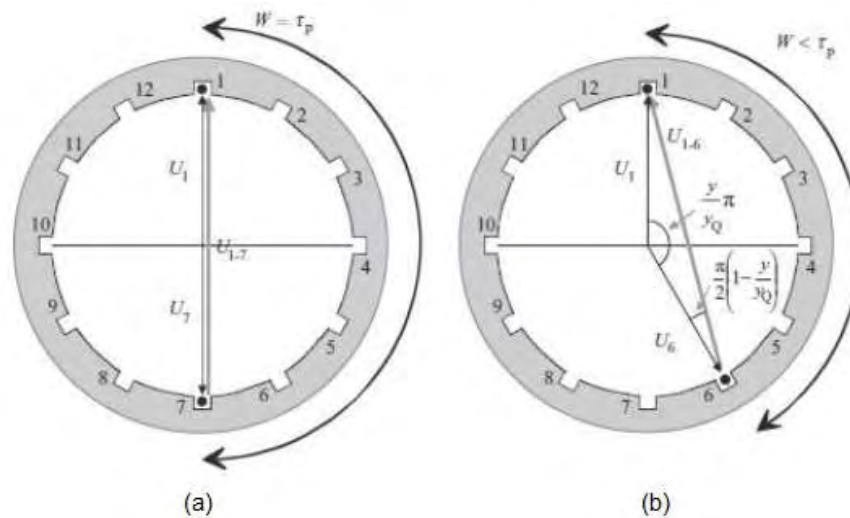


Figure 3.7: Full pitch (a) and Fractional pitch (b) windings

- **Single and Double Layer Winding**

In single layer windings, in each slot all the space is occupied by only one coil side. On the other hand, in the double layer windings, there is even number of coil sides in the same slot, dividing the slot into two layers.

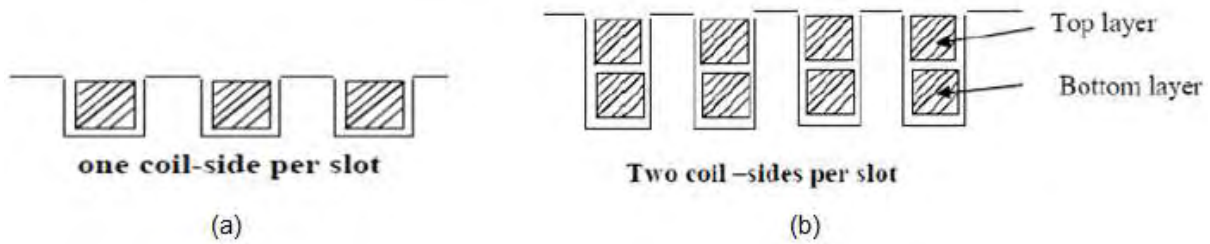


Figure 3.8: Single Layer winding (a) and Double Layer winding (b)

In the case of concentrated winding, the double layer coil will have a coil wrapped around each tooth, while in the single layer the coils will be wrapped around alternating teeth. Double layer coiling has a number of advantages over single layer winding, the use of which is limited to small machines. Some of the main advantages of the double layer winding is the ability of existence of distributed fractional winding and the easier construction and lower cost of coils.



Figure 3.9: Concentrated winding of single layer (a) and double layer (b)

- **Lap Winding**

The conductors are connected in the lap winding so that their parallel paths and poles are equal. The end of each armature coil is linked to the adjacent segment of the switch. The number of brushes is equal to the number of parallel paths in the lap winding, and these brushes are also divided into negative and positive polarities.

- **Wave Winding**

The one end of the coil is connected to the other coil's starting end, which has the same polarity as that of the first coil. The coils are connected in the shape of the wave and therefore it is called the wave winding. The conductor of the wave winding is divided into two parallel paths, and each path has specific conductors in series.

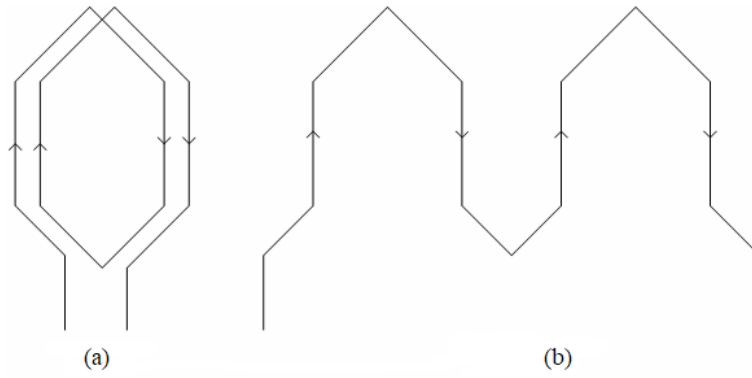


Figure 3.10: Lap winding (a) and Wave winding (b)

3.2 Principle of Induction Motors

In order to produce rotating magnetic field, Induction Motors require three phase windings and three phase currents. The three phase currents are expressed by the equations:

$$i_a = I_m \sin(\omega t) \quad (3.1)$$

$$i_b = I_m \sin(\omega t - 120^\circ) \quad (3.2)$$

$$i_c = I_m \sin(\omega t - 240^\circ) \quad (3.3)$$

Where, I_m is the amplitude and ω is the angular frequency of the applied currents.

The stator magneto-motive forces (MMFs) produced by the phase currents are given by:

$$F_a = F_m \sin(\omega t) \quad (3.4)$$

$$F_b = F_m \sin(\omega t - 120^\circ) \quad (3.5)$$

$$F_c = F_m \sin(\omega t - 240^\circ) \quad (3.6)$$

Where, $F_m = I_m \cdot N$ and N is the number of turns per phase. The resulting stator vector of the MMF is therefore expressed as:

$$F = F_a e^{j0^\circ} + F_b e^{j120^\circ} + F_c e^{j240^\circ} \quad (3.7)$$

It can be written as:

$$F = \frac{3}{2} F_m e^{j(\omega t - 90^\circ)} \quad (3.8)$$

Which is an MMF vector rotating circumferentially with the angular speed ω , and is 90° delay with respect to the MMF of phase A. In Figure 3.11 is depicted the MMF stator vectors at $\omega t = 0^\circ$ and $\omega t = 90^\circ$, verifying that the resulting MMF vector is rotating by 90° . It is equivalent to the magnetic poles of the stator, which rotates circumferentially. The angular speed is equal to the angular frequency of the phase current. If the motor has more than two poles, the speed of the rotating field is different from the angular frequency and is determined by the relation:

$$\omega_s = \frac{\omega}{p} \text{ or } n_s = \frac{f}{p} \quad (3.9)$$

Where, p is the number of pole-pairs, f is the frequency of the phase current, and ω_s and n_s are the rotating field speed (generally named as the synchronous speed) in rad/s and rev/s, respectively.

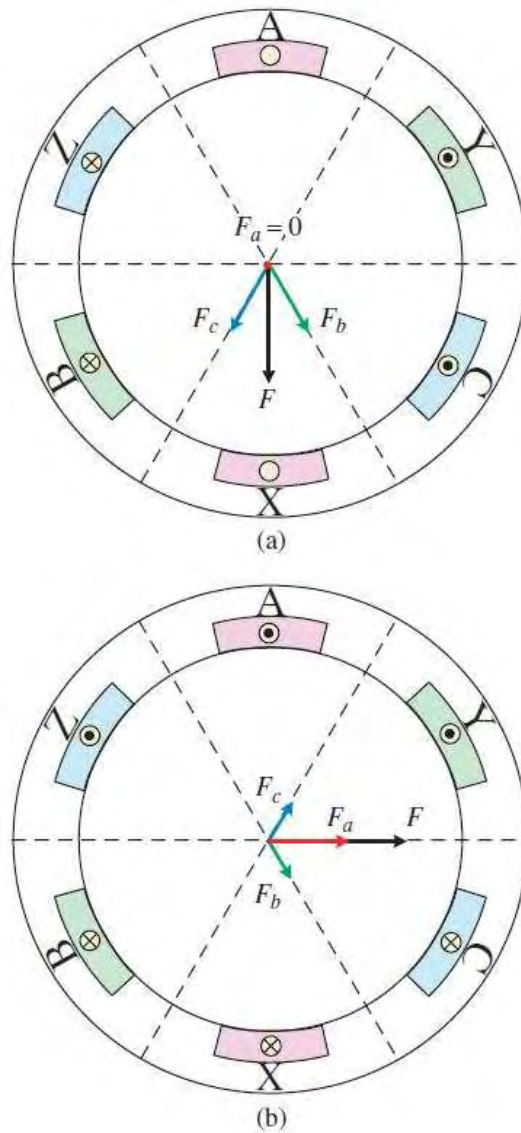


Figure 3.11: MMF stator vector: (a) $\omega t = 0^\circ$ and (b) $\omega t = 90^\circ$

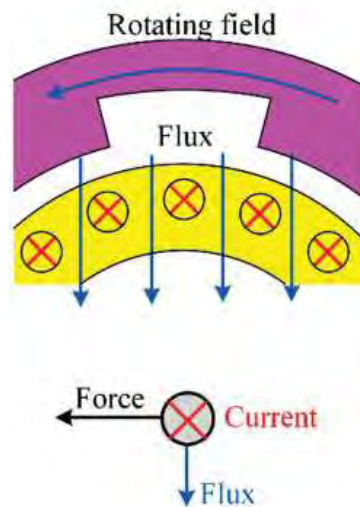


Figure 3.12: Principle of torque production

As shown in Figure 3.12, a voltage is induced in the rotor due to the relative motion that is produced by the stator's rotating magnetic field and the rotor conductors. For example, the direction of flux is downward and the field is moving from right to left. So, the produced electromotive force (EMF) and as a result the current in the conductors will be into the paper. The direction of the mechanical force is therefore to the left, which causes the conductors to follow the rotating field's moving direction and thus the driving torque. As the relative motion between the rotating field and the rotor is essential for the generation of torque, the slip s is expressed as:

$$s = \frac{\omega_s - \omega_r}{\omega_s} = \frac{\omega_{s1}}{\omega_s} \quad (3.10)$$

Where, ω_{s1} is called the slip speed, which is the relative speed between the stator's rotating magnetic field and the rotor. The induction motor works as a motor in the interval $0 < s < 1$, whereas as a generator while $s < 0$.

3.3 Modeling of Induction Motor

The principle of operation of induction motors reminds the principle of a transformer [7]. Therefore, in Figure 3.13 is depicted the basic equivalent circuit of an induction motor, where:

R_s, X_s : the winding resistance and the leakage reactance in the stator respectively

R_r, X_r : the winding resistance and leakage reactance in the rotor at standstill respectively

E_s, E_r : the induced EMF in the stator and the induced EMF in the rotor at standstill respectively

R_m, X_m : the core loss resistance and the magnetic reactance in the stator respectively

k : is the ratio of the number of stator winding turns to the number of rotor winding turns

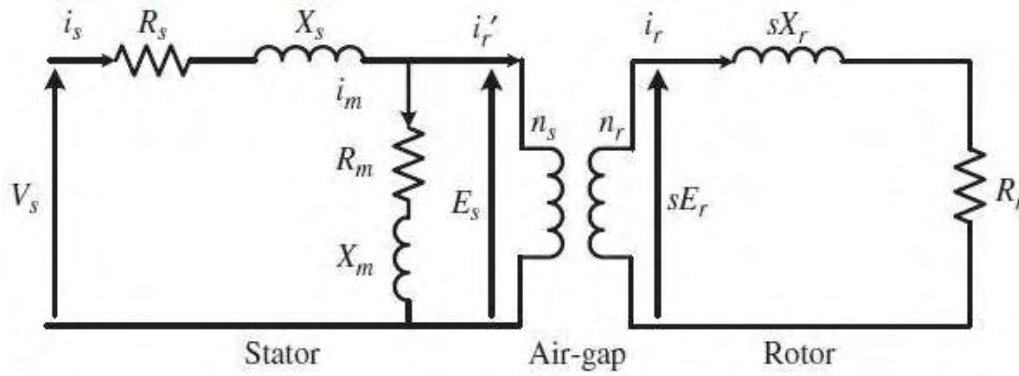


Figure 3.13: Equivalent circuit of induction motor

However, IMs stator frequency f is not equal to the rotor frequency f_r because of the existence of relative motion, which differs in a transformer. Consequently, the rotor frequency depends on the slip which is expressed by the equation $f_r = s \cdot f$. Therefore, the EMF and reactance of the rotor are both dependent on the slip and are given by $s \cdot E_r$ and $s \cdot X_r$ respectively. All rotor quantities are divided by s to simplify the IM's equivalent circuit, and then referred to the stator side. In Figure 3.14 is depicted the simplified equivalent circuit of IM, where the referred rotor quantities are expressed as: $R'_r = k^2 \cdot R_r$, $X'_r = k^2 \cdot X_r$, $E'_r = k \cdot E_r$, and $I'_r = I_r/k$. The stator, magnetizing branch, and referred impedances of the rotor are given by:

$$Z_s = R_s + jX_s \quad (3.11)$$

$$Z_m = R_m + jX_m \quad (3.12)$$

$$Z'_r = \frac{R'_r}{s} + jX'_r \quad (3.13)$$

So, the stator current and referred rotor current can be expressed as:

$$I_s = \frac{V_s}{(Z_s + Z_m \parallel Z'_r)} \quad (3.14)$$

$$I'_r = \frac{Z_m}{(Z_m + Z'_r)} I_s \quad (3.15)$$

The electromagnetic air gap power that the rotor receives from the stator is calculated as follows:

$$P_g = m \cdot I_r'^2 \cdot \frac{R_r'}{s} \quad (3.16)$$

Where, m is the number of phase. After the rotor copper loss $m \cdot I_r'^2 \cdot R_r'$ has been subtracted, the gross mechanical output power is given by:

$$P_m = m \cdot I_r'^2 \cdot \frac{R_r'}{s} \cdot (1 - s) \quad (3.17)$$

Therefore, the output torque can be calculated as:

$$T = \frac{P_m}{\omega_r} \quad (3.18)$$

Combining the Equations 3.16, 3.17 and $\omega_r = (1 - s) \cdot \omega_s$, the output torque can be re-written as:

$$T = \frac{P_g}{\omega_s} \quad (3.19)$$

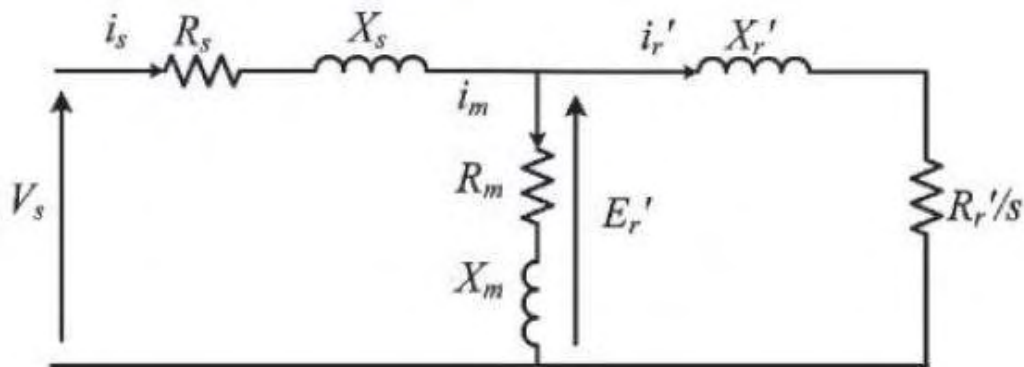


Figure 3.14: Simplified equivalent circuit of IM

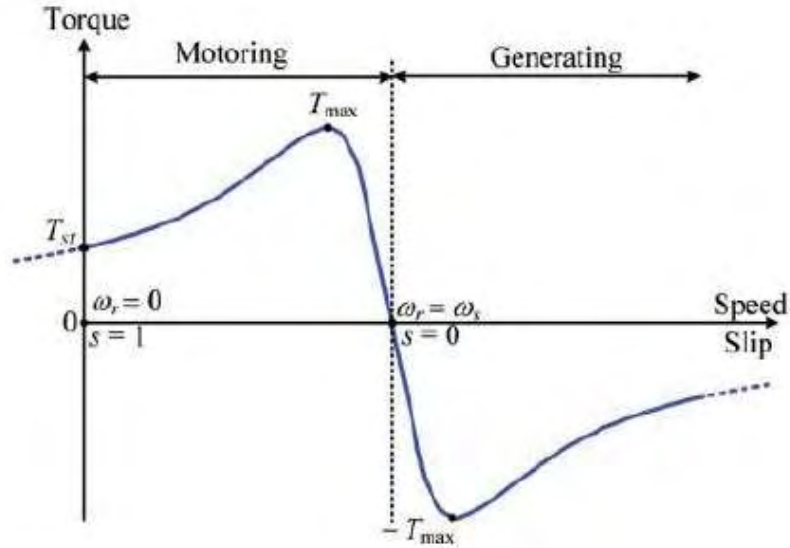


Figure 3.15: IM characteristic of torque speed

The torque equation can be simplified by neglecting the magnetizing branch as:

$$T = \frac{1}{\omega_s} \cdot \frac{m \cdot V_s^2}{(R_s + R'_r/s)^2 + (X_s + X'_r)^2} \cdot \frac{R'_r}{s} \quad (3.20)$$

Figure 3.15 shows the IM characteristic of torque speed under adjusted frequency and voltage, where T_{st} is the starting torque and T_{max} is the maximum torque. Because of the low starting torque and the limited speed range, this torque speed characteristic is clearly not good enough for EV propulsion. For EV applications, the integration of power electronics in the induction motor drive is thus almost mandatory.

3.4 Inverters for Induction Motors

The induction motor inverters are in general classified into voltage fed and current fed types [7]. Due to the need for a large inductance series to emulate a current source, the current fed inverters are rarely chosen for EV propulsion. Actually, voltage fed inverters have been extensively used, mainly for the reason of being really easy to use.

The design of the inverter depends heavily on the power device technology. The insulated gate bipolar transistor (IGBT) is currently the most desirable inverter and is broadly used by newly produced EVs. The power device selection is based on the requirements that the voltage rating is at least twice the nominal battery voltage due to the voltage surge during the switching process, the current rating is

large enough so that several power devices do not need to be connected in parallel and the switching speed is high enough to suppress motor harmonics and acoustic noise.

3.4.1 PWM Switching Inverters

Over the years, several Pulse Width Modulation (PWM) switching schemes were created for voltage fed inverters driven by the requirements that the magnitude and frequency of the basic component of the output waveform may vary smoothly, the harmonic distortion of the output waveform is minimum, the switching algorithm can be implemented in real time with minimum hardware and software, and the fluctuation of battery voltage is negligible or tolerable. The PWM switching schemes can be current controlled or voltage controlled. The use of current control is desirable for high performance IM drives, as the flux and motor torque are related directly to the controlled current. There are many PWM switching schemes for the voltage fed inverters but mostly the space vector PWM and the hysteresis current PWM schemes have been commonly used by IM drives for EV propulsion.

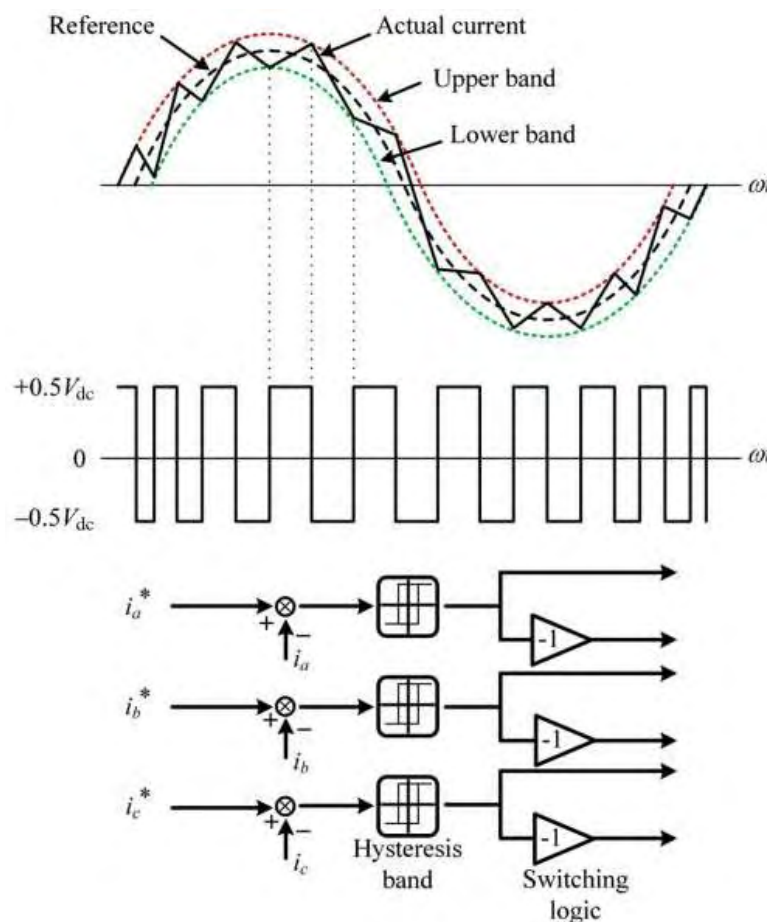


Figure 3.16: Principle of hysteresis-current PWM

The principle of hysteresis current PWM switching scheme is depicted in Figure 3.16. The actual current is calculated online and then is compared to the reference current, so that when the actual current exceeds the upper hysteresis band of the reference current, the upper switch is turned off and the current begins to decrease. At the time that the actual current meets the lower hysteresis band, the upper switch is turned on and the current begins to increase. Therefore, the actual current is forced to follow the reference current within the hysteresis band. This switching scheme has the major benefits of direct current control and quick response. However, the PWM frequency varies with the load, so that the current harmonics are not optimal but varying. In addition, the fundamental current suffers from phase lag.

3.4.2 Soft Switching Inverters

Inverters can use soft switching as an alternative instead of hard switching. Soft switching's key is to use a resonant circuit to form the current or voltage waveform, in order the power device to perform zero-current switching (ZCS) or zero-voltage switching (ZVS) to minimize the current and voltage overlap, thereby minimizing the switching loss. Generally, soft switching inverters have the following benefits:

- Improved overall efficiency
- Improved overall power density
- Reduced electromagnetic interference (EMI)
- Minimized audible noise

In contrast, soft switching inverters face the following disadvantages:

- Complex circuit
- Complex control
- Impaired reliability of the system
- Higher cost and losses

3.5 Induction Motor Control

For induction motor drives, three main types of control strategies exist: the variable voltage variable frequency control (VVVF), the field oriented control (FOC), and the direct torque control (DTC) [7].

3.5.1 Variable Voltage Variable Frequency Control

VVVF control has been extensively used for speed control of induction motor drives. For frequencies under the rated frequency, the control strategy is based on constant volts/hertz control. For frequencies beyond the rated frequency, the control strategy is based on variable frequency control with constant rated voltage. In the case of very low frequencies, voltage boosting is used to compensate for the difference between the voltage applied and the EMF induced.

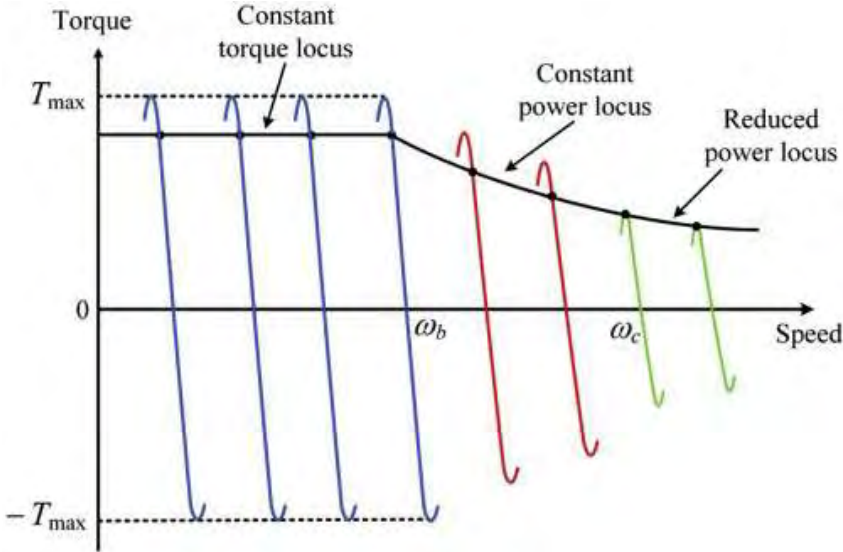


Figure 3.17: IM’s VVVF control characteristic of torque speed

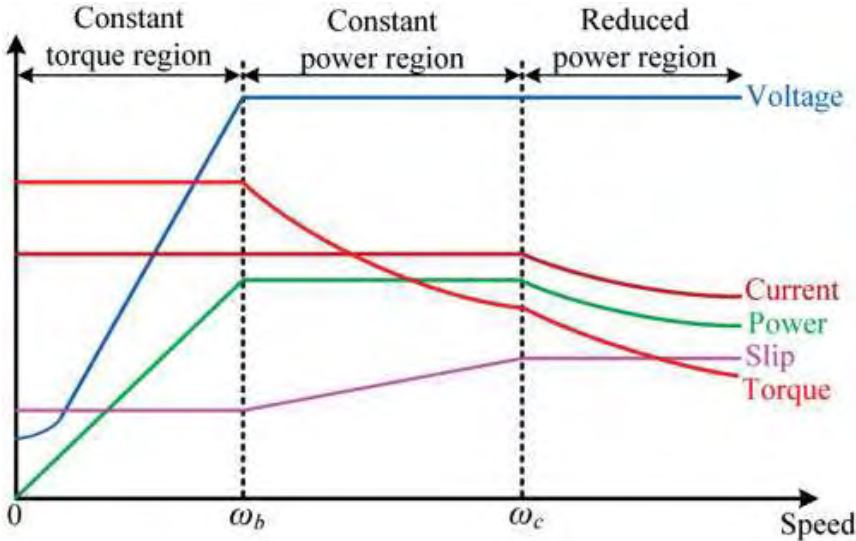


Figure 3.18: IM’s VVVF control operation

In Figure 3.17 and Figure 3.18 show the torque speed characteristics of the VVVF IM control and the torque speed operation of the VVVF control, respectively. There are three operating regions in Figure 3.18. In the first one, the motor can produce its rated torque for speeds below the rated speed (normally referred to as the base speed ω_b) and is named the constant torque region. The second is the constant power region, in which the slip is gradually increased to the maximum value, such that the current of the stator remains constant and the motor maintains its rated power capability. The third is the reduced power region, in which the torque capability decreases with the square of speed. This happens because once the speed exceeds the critical speed ω_c , the slip remains constant, while the current of the stator declines.

It must be mentioned that with the use of VVVF control, the torque and the air gap flux are functions of voltage and frequency. This connection is primarily responsible for the slow response, which means that the torque control is not accurate and quick enough to be used for high performance EVs.

3.5.2 Field Oriented Control

FOC control offers a more dynamic performance of induction motor drives, which is why is preferred to VVVF control. The concept of field oriented control (FOC), presented by Siemens tech company many years ago, is also called as transvector control, because the control implementation is based on vector transformation from rotating to stationary reference frame and vice versa.

The field oriented control (FOC) strategy allows for optimum transient drive response and has a good dynamic response. On the other hand, field orientation is a technique that provides a method for decomposing the stator current into magnetizing component I_M , which produces the flux and torque component I_T , which produces the torque. These components are then separated and individually controlled. Generally, the magnetizing component I_M varies slowly and is kept constant for quick response. The other component I_T , varies rapidly. It can be concluded that I_M varies with the magnetizing inductance and I_T with transient inductance of the machine. Thus, it provides independent torque and flux control. The magnitude and phase (vector control) of the stator currents are controlled in such a way that the flux and the torque components of current remain separated during dynamic and static conditions. The FOC for IM drive can be implemented in two ways: Direct and indirect approaches.

The direct FOC, also known as the direct vector control, is to instantly identify the rotor flux connection by measuring the air gap flux or flux estimation from the measured stator voltage and current. The Hall sensors or sensing coils can be used to measure the flux of the air gap. However, the

mounting of Hall sensors in the air gap is affected by mechanical vibration problems and temperature variations problems, which are impractical under the harsh operating environment of EVs.

The indirect FOC, also known as indirect vector control, is broadly used by IM drives for EV propulsion. The rotor flux link does not need to be identified by this technique. The key is to calculate the slip speed which is necessary to deduce the instantaneous position of the rotor flux θ_e for correct field orientation:

$$\theta_e = \int_0^t \omega_e dt = \int_0^t (\omega_{sl} + \omega_r) dt = \int_0^t \omega_{sl} dt + \theta_r \quad (3.21)$$

Where ω_e is the synchronous speed, ω_{sl} is the slip speed, ω_r is the rotor speed, and θ_r is the rotor position that is measured in real time using a position encoder.

While IM has extensively adopted indirect FOC for high performance drives, it still has some disadvantages. In particular, the rotor time constant τ_r (which also has a powerful effect on the decoupling condition) changes significantly with the operating temperature and magnetic saturation, inevitably leading to a deterioration of the desired indirect FOC. There are currently two useful ways to solve this problem. One way is to identify the rotor time constant online and update the parameters that were used in the indirect FOC controller accordingly. Another way is to adopt a sophisticated control algorithm so that the indirect FOC controller is not sensitive to variations in motor parameters.

3.5.3 Direct Torque Control

The DTC is an advanced scalar control system that can provide similar performance for the IM drive as the FOC. This scheme directly controls the connection of the stator flux and the torque by selecting the switching modes of the PWM inverter. The selection is made to limit the flux and torque errors in the respective flux and torque hysteresis bands, thus achieving flexible control and quicker torque response.

Compared to the FOC, the DTC has certain benefits for the IM drives:

- There is no need to use computationally intensive coordinate transformations.
- There is no need for current feedback control.
- The motor torque can be controlled directly, making the torque response much quicker.

The DTC, however, suffers from the disadvantages of slow response during start up and high torque ripple.

3.6 Preliminary Design

Preliminary dimensioning takes fundamental factors into account. Below are presented these magnitudes and their calculation relations in the case of the three-phase motor, based on typical values of fundamental magnetic electrical and thermal magnitudes.

3.6.1 Fundamentals Factors of Dimensioning

- **Specific Magnetic Loading**

The specific magnetic loading \bar{B} connects the number of poles P with the magnetic flux per pole Φ and equals:

$$\bar{B} = \frac{P \Phi}{\pi L D} \quad (3.22)$$

Where D is the gap length and L the axial length of the active part of the machine.

Typical values for \bar{B} are between 0.5 and 0.6T. The upper limit is set by the saturation effect of the ferromagnetic material on the stator teeth. High magnetic loading means increased ability to generate torque and power. The price is increased core losses, especially when the stator teeth are in saturation.

- **Specific Electric Loading**

The specific electric loading ac is determined by the active value of the ampere-turns (At) per meter of periphery of the gap and is defined by the relation:

$$ac = \frac{3 \cdot 2 \cdot N_s \cdot I}{\pi \cdot D} \quad (3.23)$$

Typical values of specific electric loadings range from 15000 AE / m to 45000 AE / m. The specific electric loading determines, together with the specific magnetic loading, the torque generation

capability of a given machine. As far as losses are concerned, the electric loading is associated with the machine's copper losses.

- **Apparent Power**

The apparent power is given by:

$$S = 3 \cdot e \cdot I \quad (3.24)$$

Where I is the current per phase and e the effective value of the induced voltage which is given by:

$$e = 4,44 \cdot k_w \cdot f \cdot N_s \cdot \Phi \quad (3.25)$$

Where k_w is the winding coefficient, N_s is the total number of rounds per phase, Φ is the fundamental magnetic flux per pole and f the electrical frequency which is connected to the mechanical speed of rotation n in units of turns per second with the ratio:

$$f = \frac{n \cdot P}{2} \quad (3.26)$$

By combining the above equations we finally have the three-phase apparent power:

$$S = 1,11 \cdot k_w \cdot B \cdot \pi^2 \cdot D^2 \cdot L \cdot ac \cdot n \quad (3.27)$$

As can be seen from this relation, the output power of the machine is proportional to the square of the diameter of the gap and proportional to the axial length of the active part of the core. Thus, when designing a motor or generator, the most advantageous combination of specific electrical and magnetic loading, gap dimensions and rotation speeds must be determined in order to obtain the desired output power without sacrificing other machine characteristics, such as performance, cost of the accommodation and the total weight.

- **Air Gap Voltage**

Limited gap voltage expresses the mechanical strength of the machine's rotor. It is expressed as the centrifugal force exerted on the rotor per unit area. The centrifugal force is defined by the relation:

$$F = m \cdot \omega_{rm} \cdot R \quad (3.28)$$

Where m is the mass of rotor, ω_{rm} its mechanical angular speed of rotation and R its radius. So the limited voltage of gap is expressed as:

$$\text{Air Gap Voltage} = \frac{m \cdot \omega_{rm} \cdot R}{2 \cdot \pi \cdot L} \quad (3.29)$$

The maximum permissible gap voltage is 10 tn/cm^2 . However, a safe choice is 1 tn/cm^2 . This introduces a limitation in terms of mechanical strength to the final choice of geometric dimensions of the machine.

- **Current Density of the winding**

The current density of the winding is the basic electrical size of the machine and is related to its thermal balance as it determines the volume of losses in the machine winding. In the usual case the thermal losses in the nominal operating condition are primarily losses of copper and secondly iron losses. Thermal losses cause an increase in the temperature of the machine, which can cause damage to its materials if they exceed their thermal resistance limits. Also, the insulating capacity of the insulating materials used may be degraded.

An empirical current density limit is 4 A/mm^2 , above which there is a need for forced cooling to be implemented by artificial ventilation or with a closed coolant circulation system in the case of high power engines.

3.6.2 Steps of Preliminary Design

- **Electromagnetic Torque**

Determination of the minimum surfaces of the gap is made taking into account the maximum desired gap torque. It is assumed that for the production of maximum torque, the electric angle of the stator and rotor fields is 90 electric degrees. Initially, tangential gap pressure is calculated as follows:

$$P_t = \frac{\int_C B_n \cdot B_t dl}{\pi \cdot D \cdot \mu_0} \quad (3.30)$$

Where, B_n , B_t the radial and tangential component respectively of the magnetic induction and the integral extends along the middle of the gap.

After the tangential pressure is calculated, the following expression is used to find the electromagnetic torque:

$$T_{el,max} = \frac{\pi}{2} \cdot P_t \cdot D^2 \cdot L \quad (3.31)$$



Figure 3.19: An electrical machine in which can be distinguished both the active length (L) and the diameter of the air gap (D)

- **Dimensional ratio D and L**

The dimensioning of the electrical machine air gap involves issues of performance and mechanical strength. In terms of performance, the 3.26 expression indicates that discoidal machines are preferred as the machine's power increases with the square of the gap diameter. On the other hand, the performance of the machine does not necessarily increase when the D / L ratio is increased. The reason is that in the case of a large gap diameter with respect to the length of the machine, the percentage of the winding outside the active core area rises and consequently the thermal losses are increased. Also, a machine with a very long gap has a large core mass and is expected to exhibit increased core loss, so it does not achieve optimal performance.

The mechanical strength of the rotor and the dimensioning of the gap depend on the rotor speed. At low rotation speeds, a high ratio of D / L is preferred. At high rotation speeds, the limited gap voltage limits the rotor to a small radius and the desired power is then obtained by increasing the axial length of the machine. However, in this case there is a mechanical limit in reducing the ratio of D / L , which consists in the rigidity of the body of the rotor and the maintenance of the gap.

There are some analogies that a machine needs in order to be characterized by high performance, efficiency or a balanced combination of both. Usually the ratio of the axial length of the machine L and the length of a pole τ , is important. The pole length is given by the relation:

$$\tau = \frac{\pi \cdot D}{P} \quad (3.32)$$

L / τ	Characteristic of electric machine
1.0	Balanced design
1.0 – 1.5	High power factor
1.5	High efficiency
1.5 – 2.0	Minimum cost

Table 3.2: Areas of L / τ

- **Air Gap Thickness**

Although last mentioned, the thickness of the air gap is of primary importance for achieving the desired operating characteristics of an electrical machine. The general principle is that the gap must have the smallest possible thickness, which is determined by the precise construction and the mechanical support of the rotor and stator.

3.7 Field Analysis with Finite Elements

Preliminary design of an engine provides a basic view of the required design of the engine. In addition, field analysis can give a detailed magnetic field analysis and lead to confirmation of the engine characteristics expected by the preliminary design or to the need to improve it. The field analysis provides the distribution of the magnetic field and through it, with proper processing can be calculated with accurate magnitudes such as torque and power, losses, electric current density, as well as localized areas of the core that are in saturation.

3.7.1 Magneto-static problems

Magneto-statics are called the problems in which the magnetic field is unchanged over time. In this case, the intensity of the magnetic field (H) and the density of the magnetic field (B) satisfy the relations:

$$\nabla \times H = J \quad (3.33)$$

$$\nabla \cdot B = 0 \quad (3.34)$$

It also satisfies the fundamental relationship between B and H for each material:

$$B = \mu H \quad (3.35)$$

If the material is nonlinear, such as saturated iron or alnico magnets, then the permeation μ is actually a function of B :

$$\mu = \frac{B}{H(B)} \quad (3.36)$$

Finding the magnetic field at any point in the space can be achieved by calculating the vector dynamic. The density of the magnetic field is written in function of the vector dynamic, A , as follows:

$$B = \nabla \times A \quad (3.37)$$

This definition of B always satisfies the equation (3.34). Then, (3.33) is written as follows:

$$\nabla \times \left(\frac{1}{\mu(B)} \nabla \times A \right) = J \quad (3.38)$$

For a linear isotropic mean (and assuming that $\nabla \cdot A = 0$), this equation results:

$$\nabla^2 A = -\mu J \quad (3.39)$$

In the general case, the vector dynamic is a vector of three components. However, in two dimensions, two of these three components are zero, and only the component in the vertical component changes.

The advantage of using vector dynamic is that all the conditions that must be met in the magneto-static field, are combined into an equation. If A is known, B and H are derived from A . In the case of a harmonically changing magnetic field, eddy currents can be induced in non-zero conductivity materials, and then other Maxwell equations with respect to the distribution of the electric field have to be considered.

3.7.2 Boundary Conditions

In order for the magnetic vector dynamic to be determined everywhere correctly, it is necessary to define the appropriate boundary conditions in the problem. The choice of boundary conditions not only affects the final solution but also helps to reduce the surface of the problem.

- **Dirichlet Boundary Condition**

This condition is set to the limits of the problem where the magnetic vector dynamic A has a constant value. The flow is tangent to this limit and does not penetrate it. Usually the homogeneous Dirichlet condition is used at the outer boundaries of the problem, which sets the magnetic vector dynamic $A_z = 0$. Setting this condition is equivalent to considering an external material with zero magnetic permeability, namely an insulating material.

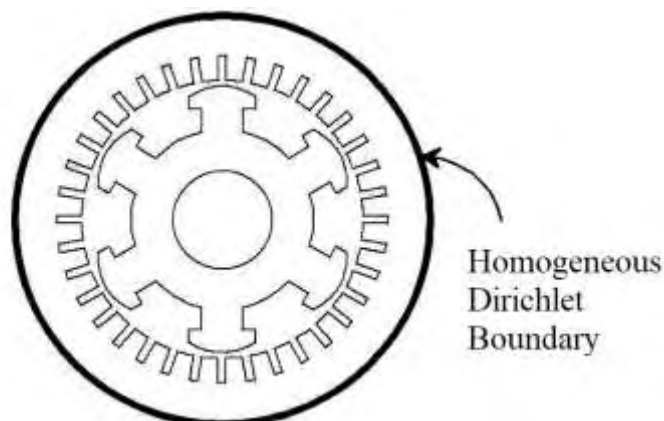


Figure 3.20: Homogeneous Dirichlet Boundary

- **Neumann Boundary Condition**

This condition is set to the limit of the problem where the derivative of magnetic vector $\partial A / \partial n$ has a constant value. That is, the flow lines have a constant gradient with the limit. The usual form of use is the points of the problem where $\partial A / \partial n = 0$, that is, where the flow lines are vertical to the boundary. When applied to a magnetic field it limits the magnetic induction B to have components only in the boundary line. Its implementation is equivalent to an interface with a very high permissible material.

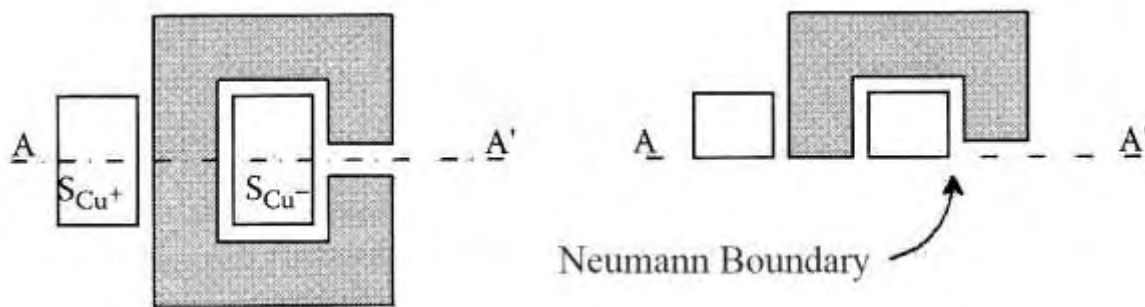


Figure 3.21: Reduction of the surface analysis using Neumann Boundary Condition.

- **Robin Boundary Condition**

This kind of boundary condition is a combination of the boundary conditions of the Dirichlet and the Neumann, defining a relation between the value of A and the vertical derivative of the boundary. The Robin boundary condition is written:

$$\partial A / \partial n + c_1 A = c_2 \quad (3.40)$$

This boundary condition is often used in finite element programs for problems with induction currents (eddy currents).

- **Periodic and Anti-periodic Boundary Condition**

The periodic condition applies to two or more lines of the boundary. With its application, the magnetic dynamic of the two lines is equal and is used at the points of the problem where the magnetic field is repeated. This way, the problem solving time is greatly reduced.

The anti-periodic condition behaves just like the periodic one with the only difference that at the two points applied it sets up a magnetic vector dynamic equal but with the opposite sign.

3.7.3 The Finite Element Method

Although the conditions of a magnetic problem can be expressed in the form of a differential equation, with some boundary conditions, it is very difficult to find an analytical solution only for problems of very simple geometry. This difficulty is overcome by the finite element analysis, dividing the problem into a large number of areas and corresponding subfields that refer to simple geometry and are easy to solve. If the initial region is fragmented into a large number of such sub-regions, the calculated potential approximates its exact value quite well. The advantage of dividing the problem area into a large number of small elements is that the problem is transformed by a small but difficult to solve problem, to a large but relatively easy to solve. This problem takes the form of a linear algebra problem with many thousands of unknowns usually, and there are algorithms that allow it to be resolved in a short time.

3.7.4 Finite Element Analysis using the FEMM program

Free FEMM software belongs to the class of finite element solver programs and solves two-dimensional and magneto-static problems, as well as problems where the magnitudes vary with a certain frequency. In particular, this program distinguishes the problem area using triangular elements. In each element, the solution is approximated by linear interpolation of the potential values at the vertices of the triangle. The linear algebra problem is formed by minimizing the magnitude of the error between the actual differential equation and the approximate differential equation.

The process of solving a magnetic problem from FEMM has the following stages:

- 1) Design of geometry, definition of boundary conditions and materials.
- 2) Gliding the problem with a desired number of triangular elements.
- 3) Solving the linear algebra problem and finding the vector potential.
- 4) Representation and processing of results

3.8 Copper Losses

Copper losses are the ohmic losses caused by the passing of current from the motor coils. As can be seen from the Ohm law, copper losses are directly proportional to the total resistance per phase and

proportional to the square of the current value of the current flowing through the coils of each phase. For a three-phase machine, the losses are given by the relation:

$$P_{cu} = 3 \cdot I^2 \cdot R \quad (3.41)$$

The existence of harmonic components in the phase current causes additional copper losses of higher grade. It is therefore important that the harmonic distortion of the current is limited in order to limit the corresponding losses of copper.

3.9 Core Losses

Precise estimation of core losses is a prerequisite for calculating engine performance. This is particularly true in the case of performance-optimized engines, because in this case core losses tend to be comparable to copper losses, so they are an important component of loss. Permanent magnet machines are one such example, because they show high performance and a high percentage of core losses over total, unlike induction motors. Core losses are the most important factor in limiting the speed of rotation in a permanent magnet machine, which implies the need to develop field weakening techniques to achieve a wide range of motion speeds [10].

When a magnetic material is in a magnetic field that varies in time, heat losses occur. These losses are called core losses. The mechanisms for converting field energy into heat are two, so the corresponding types of core losses occur: hysteresis and loss of eddy currents.

3.9.1 Hysteresis Losses

When the magnetic flux density in a medium changes, then energy is absorbed or delivered by this medium. This action is given by the integral:

$$W = \int_{B_1}^{B_2} H dB \quad (J/m^3) \quad (3.42)$$

Ferromagnetic materials tend to maintain magnetic flux in their bodies after the magnetic field has been applied, even after it has been removed. For this reason, the magnetization and demagnetization curves differ, finally forming the hysteresis loop as shown in Figure 3.22.

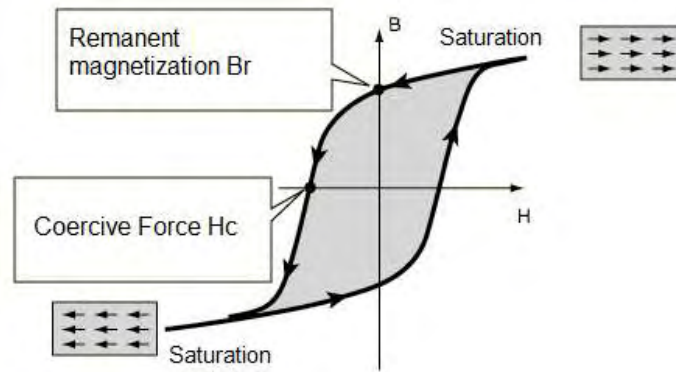


Figure 3.22: Hysteresis Loop

By calculating the above integral for a complete cycle of magnetization and demagnetization, the material absorbs more energy than it produces. The energy difference is converted into heat and is equal to the area of the hysteresis loop. This energy lost in each cycle is called the loss of hysteresis and occurs throughout the bulk of the material, resulting in increased temperature and reduced performance, be it a transformer or an electrical machine.

In the specific case where the magnetic flux changes sinusoidally with frequency f , without the formation of smaller loops and with a maximum value B_m , the empirical relation gives the specific loss of delay [11]:

$$p_h = k_h \cdot f \cdot B_m^x \quad (W/m^3) \quad (3.43)$$

Where, k_h constant that depends on the structure of the material and x the Steinmetz constant ranging between 1.8 and 2.2, usually taken as 2.

The above modeling of hysteresis losses assumes that the magnetic flux changes only in the measurement, while its address remains constant. This situation happens in transformers, most of their core. In the rotating machines, however, there is a change in the direction of the magnetic flux. As a result, more rotary loss of hysteresis occurs in electrical machines.

3.9.2 Eddy Current Losses

The temporal change in magnetic flux induces a field in the body of the core. Due to the conductivity of the ferromagnetic materials, there are currents in the body of the core, called eddy currents, which

flow cyclically in a plane perpendicular to the direction of the magnetic flux. Therefore, Joule losses occur and part of the energy of the field is transformed into heat.

In the case where the magnetic flux changes sinusoidally in terms of its measure alone, a description of the specific loss of eddy currents is as follows:

$$p_e = k_e \cdot f^2 \cdot B_m^2 \quad (W/m^3) \quad (3.44)$$

Where, k_e constant depends on the properties of the material and f is the frequency of change of the magnetic field. As mentioned earlier, if the direction is changed, the loss of eddy currents is greater.

3.10 Induction Motor Classes

Three-phase IMs are classified by their type of electrical design. The motors have been specified in the design categories A, B, C and D by NEMA (National Electrical Manufacturers Association). These designs are suitable for specific classes of applications based on the typical load requirements of each class. The torque of the motor varies with the speed, as it operates from no load to full load. The graph which is called a speed-torque curve, displays the relation between speed and torque. This curve illustrates the torque of the motor, as a percentage of full load torque, over the full speed range of the motor, which is depicted as a percentage of motor's synchronous speed. The classification of NEMA is based on the curves of speed-torque. The characteristic speed-torque curve for designs A, B, C, and D is depicted in Figure 3.23.

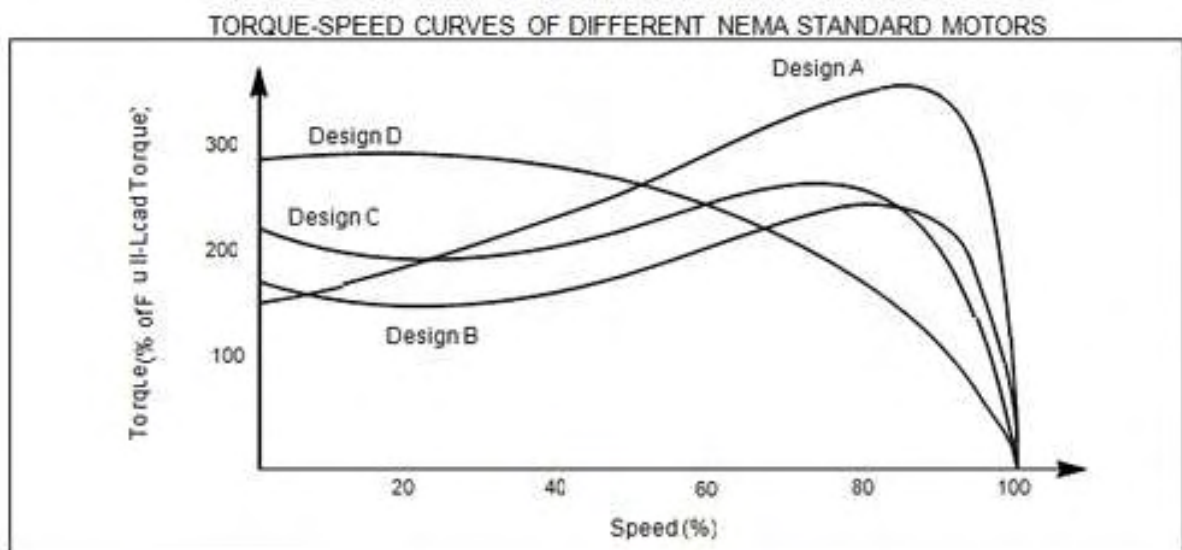


Figure 3.23: Torque - Speed curves of NEMA Classifications for Induction Motors

- **Design A** has normal starting torque (typically 150-170% of rated) and relatively high starting current. The breakdown torque is the highest of all the NEMA types. It can handle heavy overloads for a short duration. The slip is $\leq 5\%$. A typical application is the powering of injection molding machines.
- **Design B** is the most common type of three phase AC induction motor design. It has a normal starting torque, similar to Design A, but offers low starting current. The locked rotor torque is good enough to start many loads encountered in the industrial applications. The slip is $\leq 5\%$. The motor efficiency and full-load PF are comparatively high, contributing to the popularity of the design. The typical applications include pumps, fans and machine tools.
- **Design C** has high starting torque (greater than the previous two designs, say 200%), useful for driving heavy breakaway loads like conveyors, crushers, stirring machines, agitators, reciprocating pumps, compressors, etc. These motors are intended for operation near full speed without great overloads. The starting current is low. The slip is $\leq 5\%$.
- **Design D** has high starting torque (higher than all the NEMA motor types). The starting current and full-load speed are low. The high slip values (5-13%) make this motor suitable for applications with changing loads and subsequent sharp changes in the motor speed, such as in machinery with energy storage flywheels, punch presses, shears, elevators, extractors, winches, hoists, oil-well pumping, wire-drawing machines, etc. The speed regulation is poor, making the design suitable only for punch presses, cranes, elevators and oil well pumps. This motor type is usually considered a "special order" item.
- Recently, NEMA has added one more design in its standard for the induction motor. **Design E** is similar to Design B, but has a higher efficiency, high starting currents and lower full-load running currents.

Below are the tables with the typical characteristics of all NEMA classes.

Basic Characteristics	<ul style="list-style-type: none"> • High locked rotor torque • High locked rotor current
Locked Rotor Torque (% of Full-load Torque)	70 - 275%
Pull - Up Torque (% of Full-load Torque)	65 - 190%
Breakdown Torque (% of Full-load Torque)	175 - 300%
Locked Rotor Current (% of Full-Load Current)	-
Slip	0.5 - 5%
Areas of Application	Fans, blowers, centrifugal pumps and compressors, motor-generator sets, etc., where starting torque requirements are relatively low
Efficiency	High or Medium

Table 3.3: Typical characteristics of all NEMA A class motors.

Basic Characteristics	<ul style="list-style-type: none"> • Normal locked rotor torque • Normal locked rotor current
Locked Rotor Torque (% of Full-load Torque)	70 - 275%
Pull - Up Torque (% of Full-load Torque)	65 - 190%
Breakdown Torque (% of Full-load Torque)	175 - 300%
Locked Rotor Current (% of Full-Load Current)	600 - 700%
Slip	0.5 - 5%
Areas of Application	Fans, blowers, centrifugal pumps and compressors, motor-generator sets, etc., where starting torque requirements are relatively low
Efficiency	High or Medium

Table 3.4: Typical characteristics of all NEMA B class motors

Basic Characteristics	<ul style="list-style-type: none"> • High locked rotor torque • Normal locked rotor current
Locked Rotor Torque (% of Full-load Torque)	200 - 285%
Pull - Up Torque (% of Full-load Torque)	140 - 195%
Breakdown Torque (% of Full-load Torque)	190 - 225%
Locked Rotor Current (% of Full-Load Current)	600 - 700%
Slip	1 - 5%
Areas of Application	Conveyors, crushers, stirring motors, agitators, reciprocating pump and compressors, etc., where starting under load is required
Efficiency	Medium

Table 3.5: Typical characteristics of all NEMA C class motors

Basic Characteristics	<ul style="list-style-type: none"> • Normal locked rotor torque • High slip
Locked Rotor Torque (% of Full-load Torque)	275%
Pull - Up Torque (% of Full-load Torque)	-
Breakdown Torque (% of Full-load Torque)	275%
Locked Rotor Current (% of Full-Load Current)	600 - 700%
Slip	5 - 8%
Areas of Application	High peak loads with or without flywheels such as punch presses, shears, elevators, extractors, winches, hoists, oil-well pumping and wire-drawing motors
Efficiency	Low

Table 3.6: Typical characteristics of all NEMA D class motors

Basic Characteristics	<ul style="list-style-type: none"> • Normal locked rotor torque • Normal locked rotor current • Low slip
Locked Rotor Torque (% of Full-load Torque)	75 - 190%
Pull - Up Torque (% of Full-load Torque)	60 - 140%
Breakdown Torque (% of Full-load Torque)	160 - 200%
Locked Rotor Current (% of Full-Load Current)	800 - 1000%
Slip	0.5 - 3%
Areas of Application	Fans, blowers, centrifugal pumps and compressors, motor-generator sets, etc., where starting torque requirements are relatively low
Efficiency	High

Table 3.7: Typical characteristics of all NEMA E class motors

Chapter 4

Permanent Magnet Brushless Motors

Permanent magnet (PM) motor drives, are at present the most attractive choice for electric vehicle propulsion. In fact, they hold a dominant market share of EV motor drives right now. Their main attributes, that is high efficiency and high power density, are achieved by using high energy permanent magnet materials. However, these motor drives still have some drawbacks.

The major advantages that made PM brushless machines overthrow induction machines, are the follows:

- Higher power density
- Higher efficiency
- Easier to cool
- Higher reliability
- Better dynamic response

However, the main drawbacks of these machines are:

- Machine cost is higher
- Constant power has limited range
- Demagnetization of the magnets

The PM brushless machines consist two categories of machines: the PM synchronous machine (PMSM or BLAC) and the PM brushless DC electric machine (BLDC). The PMSMs have been extensively favored for EV propulsion, while the BLDC motors are now becoming attractive.

4.1 Permanent Magnet Materials

Permanent magnet materials are essential for permanent magnet brushless motor drives as they are responsible for the lifelong excitation. The progress of PM materials has taken place step by step, as shown in Figure 4.1, and before a new one was replaced each PM material has been developed and improved. Specifically, the energy product met a radical development starting from the 1980s.

Below, there are the four main types of PM materials that are widely used for motor drives:

- *Ferrite*: The ferrite magnet was invented in the 1930s. It has been widely used as commercial magnets for the last few decades because of the abundance of raw materials and low production cost. It also offers the advantage of high electrical resistance, which can suppress the corresponding eddy-current loss. However, it suffers from drawbacks such as high temperature coefficient and low energy density, leading to be sensitive to temperature variations and bulky in size, respectively, for application to PM machines.

- *Alnico*: It is a nickname of iron-based aluminum-nickel-cobalt (Al-Ni-Co) alloy, which was invented in the 1940s. It was the first modern PM material offering high remanence. Because of its high Curie temperature, it can be used at high operating temperature. Unfortunately, its coercivity is very low so that it is very easy to be demagnetized, which limits the corresponding application to PM machines. Nevertheless, some special machines, such as the memory machine, positively utilize this property so that the magnetization level can be online tuned.

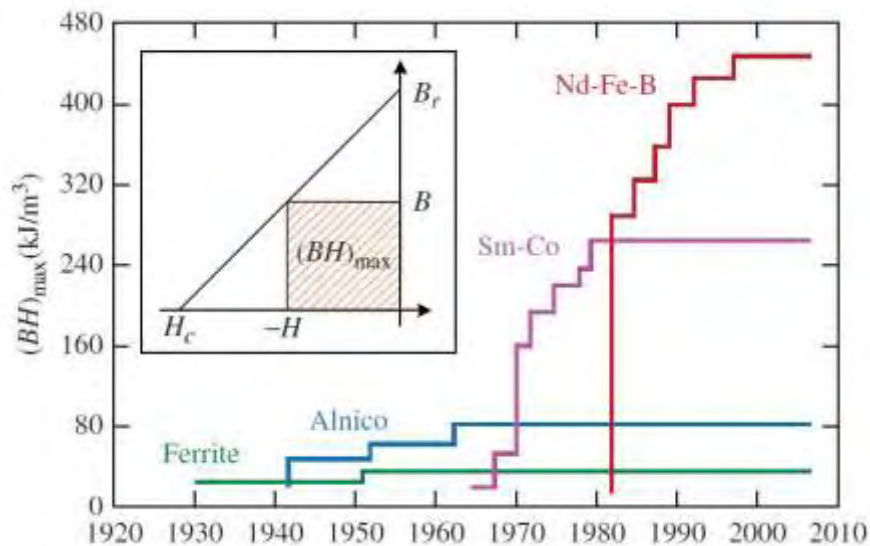


Figure 4.1: Development of PM materials (Energy Density / Time)

- *Samarium-cobalt (Sm-Co)*: Invented in the 1960s, this rare-earth PM material has merits such as high remanence, high coercivity, high energy density, high Curie temperature, and low temperature coefficient. It is well suited for application to PM machines, which desire high power density, high efficiency, and high stability. However, its cost is the key drawback. Particularly, the rare-earth element, samarium, is very expensive.

- *Neodymium-iron-boron (Nd-Fe-B)*: First produced in 1984, this rare-earth PM material has better magnetic properties than samarium-cobalt. Since neodymium is a relatively less expensive rare-earth element, the corresponding cost becomes reasonable for application to PM machines. The relatively

low Curie temperature (345°C) is the major concern, which limits its use for high-temperature applications. Currently, this PM material is almost exclusively used for EV motor drives. Because of such an exponential growth in demand, the price is highly volatile, sometimes unreasonably expensive.

In Table 4.1 are shown the typical demagnetization characteristics of the aforementioned PM materials. The remanence B_r indicates the strength of the produced magnetic field, and the coercivity H_c indicates the resistance to becoming demagnetized. The maximum energy product $(BH)_{max}$ represents the related energy density. Moreover, the attributes of PMs are generally affected from temperature. The exposure of PMs to the Curie temperature T_c has as a result the total loss of PM's material magnetization. Consequently, it is crucial to take into account the correct operating temperatures when designing PM motors.

	Ferrite	Alnico	Sm-Co	Nd-Fe-B
Remanence, B_r (T)	0.43	1.25	1.21	1.47
Coercivity, H_c (kA/m)	330	51	796	820
Energy product, $(BH)_{max}$ (kJ/m ³)	35	44	271	422
Temperature coefficient of B_r (%/°C)	-0.18	-0.02	-0.03	-0.11
Temperature coefficient of H_c (%/°C)	0.2	0.01	-0.22	-0.65
Curie temperature, T_c (°C)	450	860	825	345

Table 4.1: Properties of PM materials

The materials which can retain their magnetism are called hard magnet materials. Materials such as cobalt, iron and nickel retain their magnetism and are known as ferromagnetic materials. The most common materials that are used in electric machines are samarium cobalt and neodymium-type magnets.

The demagnetization characteristic of the four major permanent magnet types mentioned earlier is shown below:

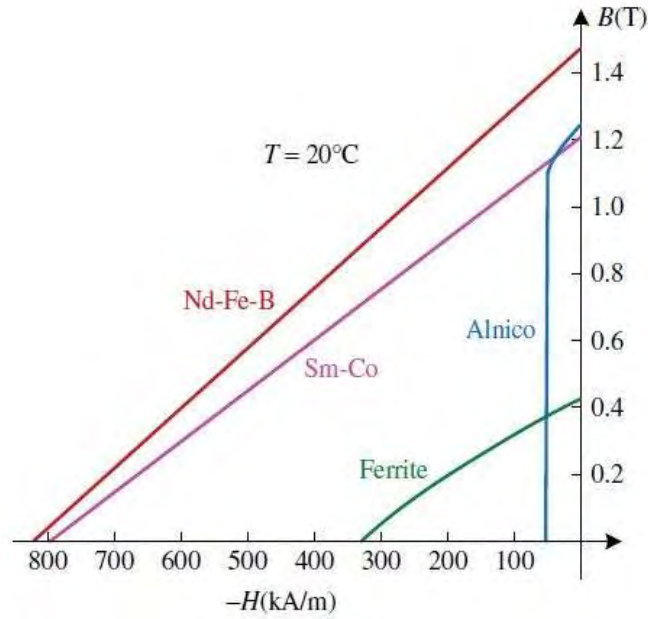


Figure 4.2: Demagnetization curves of PM materials

4.2 Permanent Magnets

The density of magnetic flux on magnets can be seen as a result of two components. One component is intrinsic and depends on the permanent alignment of the crystal domains in an applied field during magnetization. The intrinsic flux density B_i , saturates at specific intensity of magnetic field and does not increase when the intensity of the applied field increase. The other component is the excitation B_h and exists due to the intensity of the magnetic field of the magnet when the material is not under the influence of an externally applied magnetic field. As a result, the flux density in the magnet material is given by:

$$B_m = B_h + B_i \quad (4.1)$$

The excitation component B_h is directly proportional to the intensity of the magnetic field H and is given by the relation:

$$B_h = \mu_0 \cdot H \quad (4.2)$$

The excitation component is very small compared to the other component of flux density, in all magnetic materials. Combining the above equations (4.1 & 4.2), the magnetic flux density is presented as:

$$B_m = B_i + \mu_0 \cdot H \quad (4.3)$$

A typical ceramic magnet's magnet flux density can be represented in general as:

$$B_m = B_r + \mu_0 \cdot \mu_{rm} \cdot H \quad (4.4)$$

Where μ_{rm} is magnet's relative permeability. For $H = 0$, both normal induction flux density and intrinsic density go through the point identified as remanent flux density B_r . Combining the equations 4.3 and 4.4, the intrinsic flux density in the second quadrant is given by:

$$B_i = B_m - \mu_0 \cdot H = B_r + \mu_0 \cdot H \cdot (\mu_{rm} - 1) \quad (4.5)$$

It should be noted that for a hard magnet with a straight demagnetization curve, the intrinsic flux density is constant in the second quadrant, which means the magnet remains “permanently magnetic” and is considered as a high grade magnet. If the demagnetization curve is not a straight line in the second quadrant, the intrinsic flux density is not constant, which means that the magnet does not maintain its permanent magnetism and is considered a permanent magnet of low grade.

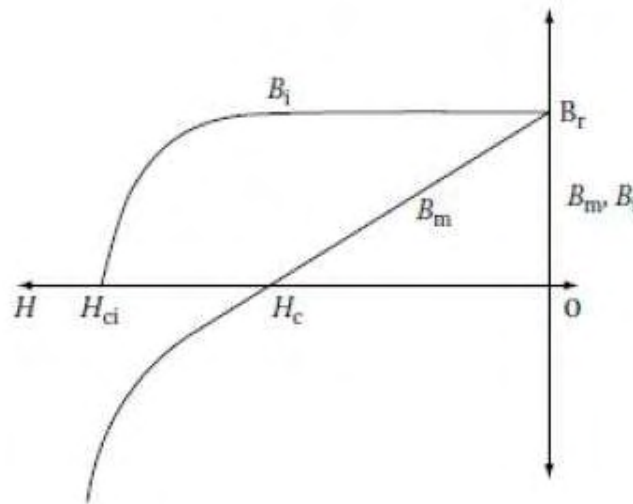


Figure 4.3: Magnetic flux density of a typical ceramic magnet

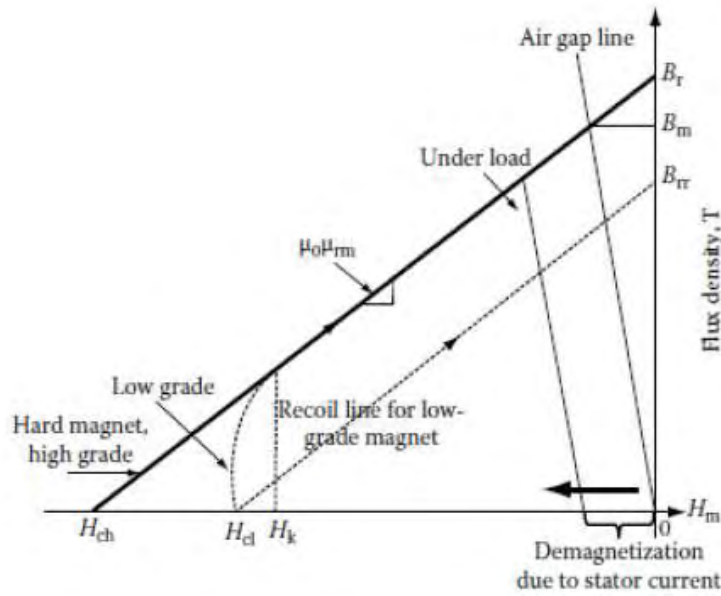


Figure 4.4: Operating Point of PMs

4.3 Operating Point and Air Gap Line

A close study of the flux path in the motor helps to identify the operating point on the demagnetization characteristic of the magnet. The flux goes from the north pole of the rotor magnet to stator through an air gap and then the flux path drives from stator to rotor south pole, again through the air gap. Therefore, the flux path includes twice the length of the magnet and twice the length of the air gap, as it is depicted in Figure 4.5. The MMF obtained by magnets equals the MMF that is supplied by the air gap, provided that the MMF of the stator and rotor is negligible. So

$$H_m \cdot l_m + H_g \cdot l_g = 0 \quad (4.6)$$

H_m , l_m intensity of the magnetic field and length, respectively, of the magnet

H_g , l_g intensity of the magnetic field and length, respectively, of the air gap

The operating flux density on the demagnetization characteristic, provided that is a straight line, is given by:

$$B_m = B_r + \mu_0 \cdot \mu_{rm} \cdot H_m \quad (4.7)$$

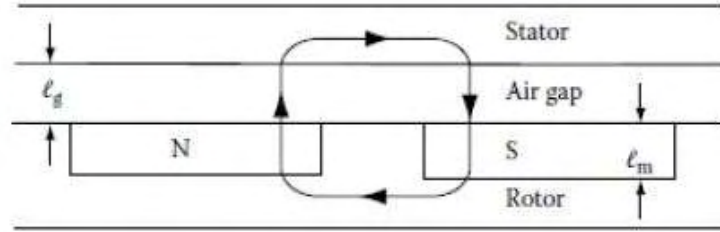


Figure 4.5: Simple layout of flux path in electric machine

The air gap flux density in terms of its magnetic field density is:

$$B_g = \mu_0 \cdot H_g \quad (4.8)$$

Using the Equations 4.6 and 4.7, the following equation is given:

$$\begin{aligned} B_m &= B_r + \mu_0 \cdot \mu_{rm} \cdot H_m = B_r - \mu_0 \cdot \mu_{rm} \cdot \frac{H_g \cdot l_g}{l_m} \\ &= B_r - \mu_{rm} \frac{l_g}{l_m} \cdot \mu_0 \cdot H_g \\ &= B_r - \mu_{rm} \cdot \frac{l_g}{l_m} \cdot B_g \end{aligned} \quad (4.9)$$

Neglecting leakage flux results in:

$$B_g = B_m \quad (4.10)$$

Finally, substituting Equation 4.9 into Equation 4.10, equation 4.11 is derived:

$$B_m = \frac{B_r}{\left(1 + \frac{\mu_{rm} \cdot l_g}{l_m}\right)} \quad (4.11)$$

It is clear from Equation 4.11 that the magnetic flux density corresponding to the operating point is always less than the remanent magnetization and is due to the excitation condition of the air gap. Also, it should be noted that iron's leakage flux and excitation requirements are ignored during this concept. The resulting equation is used for the design. Considering the case which the magnetic flux density of the air gap is equal to the remaining magnetic flux density of the magnet, the denominator of the equation has to be the one, resulting in a magnet thickness much greater than the length of the air gap with the relative magnetic permeability of the magnet. Considering a relative magnetic permeability approximately equal of high grade magnet to be 1, the thickness of the magnet will have

to far exceed the length of the air gap. This would result in a large magnet, which is not possible for a practical machine because it involves a large cost and a non-compact rotor, hence a machine as a whole, not compact. Furthermore, an additional parameter that makes this impossible is the leakage fluxes between the magnets in the air gap, which will increase as smaller is the length of the air gap compared to the length of the magnet. Thus, the practical ratio between the thickness of the magnet and the air gap length should be limited from 1 to 20. The lower this ratio, the volume of the magnet and cost will be lower and also the power output and power density of the machine. The higher this ratio, more intense the characteristics described earlier will be. Increasing the ratio does not increase the gains relative to the output power and past a certain ratio value, leakage flux and weight of the rotor product lower power density of the machine. The operating point taken from Equation 4.11 is depicted in Figure 4.4 and the line connecting the magnetic flux density B_m to the beginning of the axes is called air gap line or load line. The slope of this curve equals the negative value of a theoretical permeance coefficient μ_c , per air permeability. If the stator is electrically excited to produce demagnetization, then the air gap line shifts to the left and parallel to the air gap line, as depicted in Figure 4.4. The flux density of the operating point is further reduced in relation to B_m . The permeability coefficient is obtained for an operating point denoted by B_m and H_m as:

$$B_m = B_r + \mu_0 \cdot \mu_{rm} \cdot H_m = -\mu_0 \cdot \mu_c \cdot H_m \quad (4.12)$$

Where H_m is the intensity of the magnet field due to stator current excitation in the motor. Consequently, the permeance coefficient is given by:

$$\mu_c = -\frac{B_r}{\mu_0 \cdot H_m} - \mu_{rm} \quad (4.13)$$

The remanent flux density B_r can be expressed as a function of operating magnetic field intensity H_m :

$$B_r = -\mu_0 \cdot \mu_{rc} \cdot (H_m) \cdot H_m \quad (4.14)$$

Where $\mu_{rc} \cdot (H_m)$ is external permeability and dependent on H_m . From Equations 4.13 and 4.14 the permeance coefficient is related as:

$$\mu_c = \mu_{rc} \cdot (H_m) - \mu_{rm} \quad (4.15)$$

This μ_c formulation clearly shows the variations in the residual flux density due to changes in temperature and the impact of the applied magnetic field intensity, both of which are induced by external operating conditions. Since the demagnetizing field is introduced by external operating

conditions, the permeance coefficient decreases as the external permeability for this operating point also decreases. The external permeability of hard PMs in the nominal operating region is in the order of 1-10.

4.4 Effect of External Magnetic Field Intensity

Due to the excitation of its armature windings in the stator, PM motors experience a magnetic field in addition to the field due to PMs on the rotor. Depending on whether the fields are in the same or opposite direction, the interaction of these fields has a certain effect. External excitation (due to the winding excitation) is always meant to weaken the air gap flux. The flux is therefore directed in the opposite direction to that of the PM rotor flux due to external excitation. It is not usual to cumulatively compound the fluxes, as it would strengthen the air gap and thus lead to the saturation of the core laminations of the stator and therefore to higher core losses. The main point for not allowing the cumulative compounding of fluxes is that the magnet flux alone during the design phase of the electrical machine provides the operating point near the knee point in the lamination material characteristics of the B-H (or equivalent flux versus current). The operating point is saturated by any further compounding of the flux with external excitation.

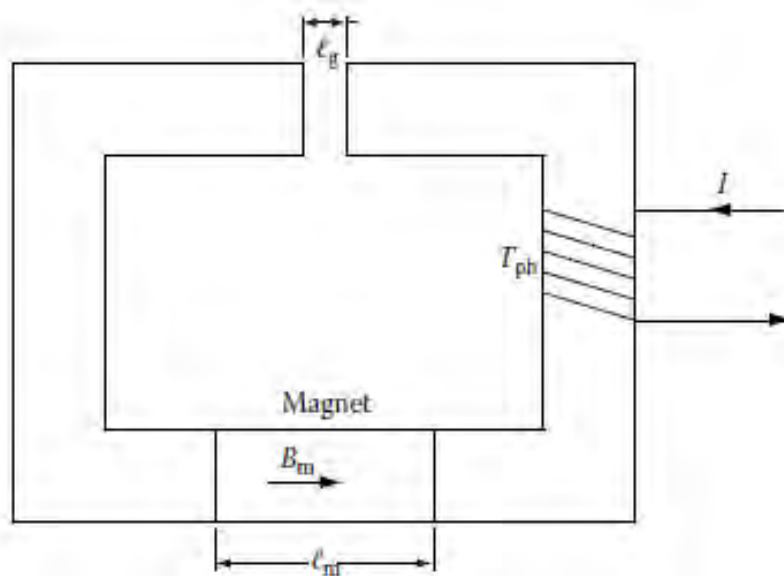


Figure 4.6: Simple electromagnetic device with a PM

To illustrate the effect of external magnetic field intensity, consider a simple electromagnetic device shown in Figure 4.6. The coil has turns T_{ph} and carries a current I . Suppose that the external current is zero ($I = 0$) and therefore there is only the PM field. In the anti-clockwise direction, a flux would

circulate in the core as the magnet polarity is defined from left to right. If the winding is excited by a current, the flux it produces will pass through the core in the same direction as the PM flux. This would increase the core and air gap flux, as the two fluxes are additive due to the winding excitation and the PM field. If the current direction in the winding is opposite to that shown in the figure, the external field is opposed to the PM flux due to the winding flux, which results in a net reduction in the flux in the core and air gap.

4.5 Arrangement of Permanent Magnets

There are many different types of magnets that can be selected for application to an electric motor. Magnets could be made even in the shape of a ring with any desired orientation of the dynamic lines, which would be perfectly applied to the rotor. However, the cost of such a construction would be unprofitable. In a construction, it is important to make decisions based on techno-economic criteria and not on purely technical criteria.

On a pole, both a single piece of magnet and many magnets could be placed together in order to achieve the desired magnetic loading. Also, many magnets can be placed on top of each other. In this case there may be magnets of different sizes, but they should always have the same magnetization direction. In Figure 4.7, the three different ways of placing magnets on a pole can be distinguished.

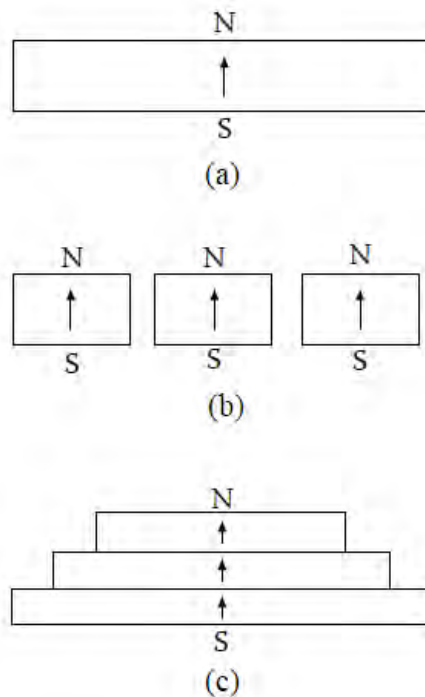


Figure 4.7: Ways that magnet can be placed on poles (a) single segment, (b) multiple segments, (c) top of each other

Each magnet placing presents advantages and disadvantages, respectively. In the case of a low power machine, a single segment permanent magnet is usually preferred. Greater power machines are usually built with multisegment magnets per pole or stack structure. In either case, both types are widely used.

Apart from the way the magnets are placed on the rotor, they can have different shapes. Figure 4.8 shows magnets with (a) rectangular shape, (b) radial shape, and finally (c) breadloaf shape. It is easily understood that the radial shape shows the best and more even distribution of the field in the gap. As far as rectangular magnets are concerned, when cut into large individual pieces, they are usually placed inside the rotor in holes that are made during or after construction.

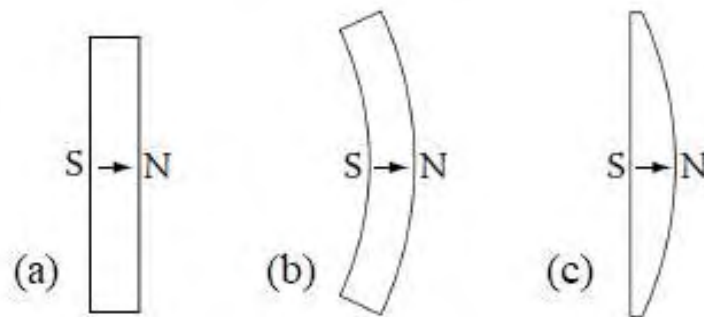


Figure 4.8: Different shapes of permanent magnets (a) rectangular, (b) radial, (c) breadloaf

There are many ways in which the magnets could be placed or designed according to their imagination and the application they wish to implement, yet such construction should be carried out in accordance with the following criteria [8]:

- Minimum material per magnet pole
- Ease of placement, processing and construction
- Flux density distribution that is rectangular or sinusoidal

4.6 Magnetization of Permanent Magnets

Permanent magnets are magnetized by the manufacturer in a certain orientation or direction. The direction of magnetization is a factor that should be taken seriously into account as, among other things, it greatly affects both the magnetic flux distribution and the power density for various geometries. The air gap flux density distribution affects the production of harmonic torque in the machine and the existence of harmonic torques degrades the quality of the torque output in the

machine, especially in terms of high performance motor drives. Radial and parallel magnetizations are established in practice while other forms are not near yet.

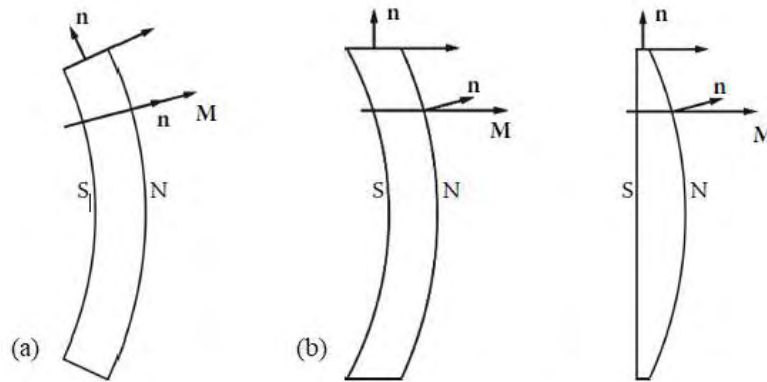


Figure 4.9: (a) Radial and (b) Parallel magnetizations

In Figure 4.9, both types of magnetization are distinguished, where vector n indicates the normal direction to the surface and M indicates the magnetization vector. Figure 4.10 shows the distribution of magnetic lines as well as the magnetic induction in the air gap for the two different ways of magnetization for a bipolar machine with 24 slots in the stator. The radially magnetized magnets generate a rectangular distribution of flux density in the air gap, while the parallel magnetized magnets generate a sinusoidal distribution of flux density in the air gap.

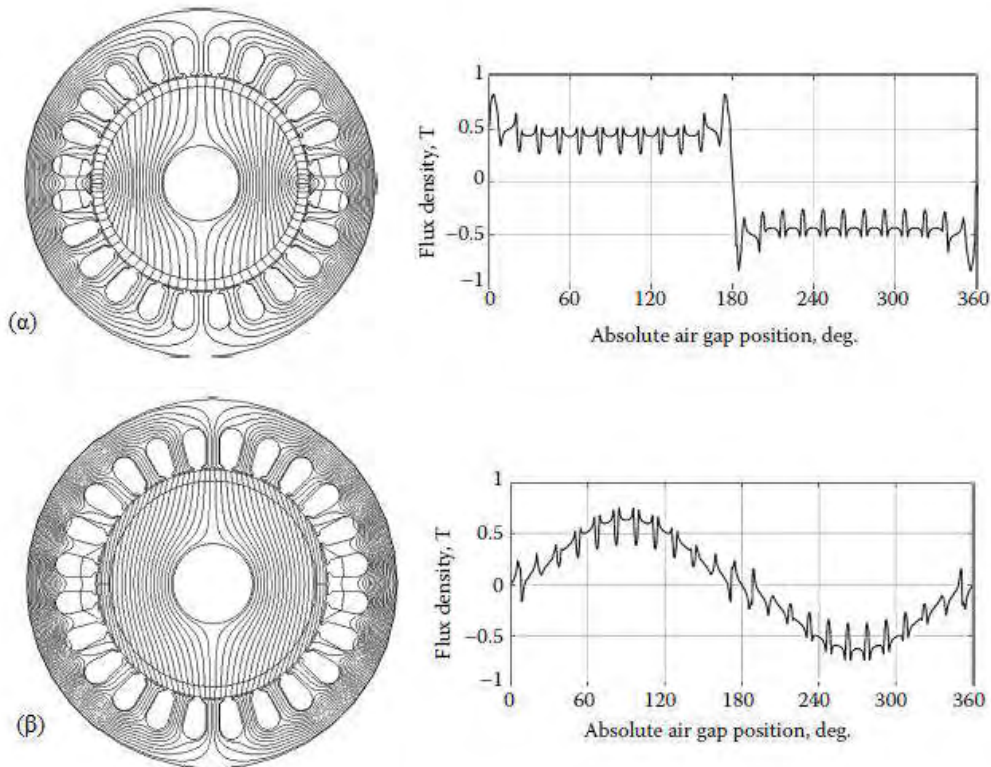


Figure 4.10: Magnetic lines and magnetic induction in the air gap for (a) machine with radial magnetization, (b) machine with parallel magnetization

4.7 Structure of Permanent Magnet Brushless Motors

The basic structure of the Permanent Magnet Brushless Motor is shown in Figure 4.11. It mainly consists of a stator with a three phase armature winding and a rotor with attached permanent magnets. The existence of PMs instead of using an armature winding in the rotor, offers the benefit of not requiring energy expenditure on excitation windings, as is the case with induction motors. This structure applies both to PMSM and BLDC types. The designing procedure of the stator and the materials that are used in order to be made, do not differ from the case of induction motors that is already mentioned in chapter 3.

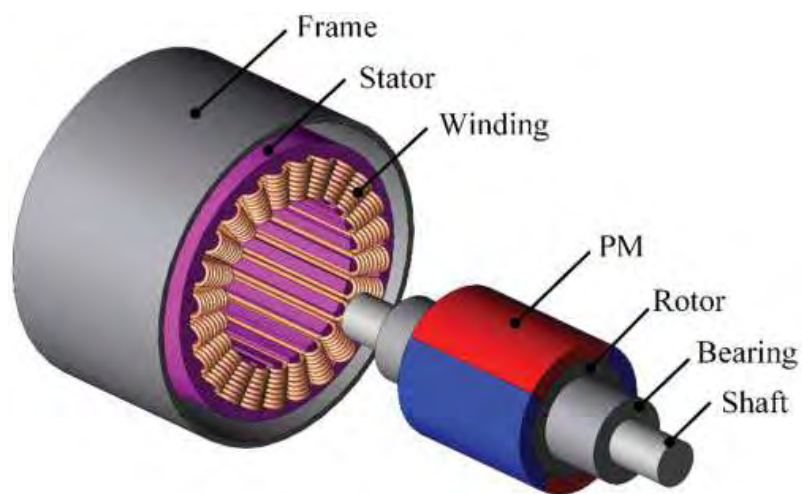


Figure 4.11: PM brushless motor exploded diagram

4.7.1 Permanent Magnet Rotor Types

Several PM rotor topologies were developed to adapt their attributes to the specific application for which they were intended. The general categories of machines are divided by placing permanent magnets on the rotor and by placing the rotor itself. The Permanent Magnet Brushless motors are therefore classified analytically according to the following categories.

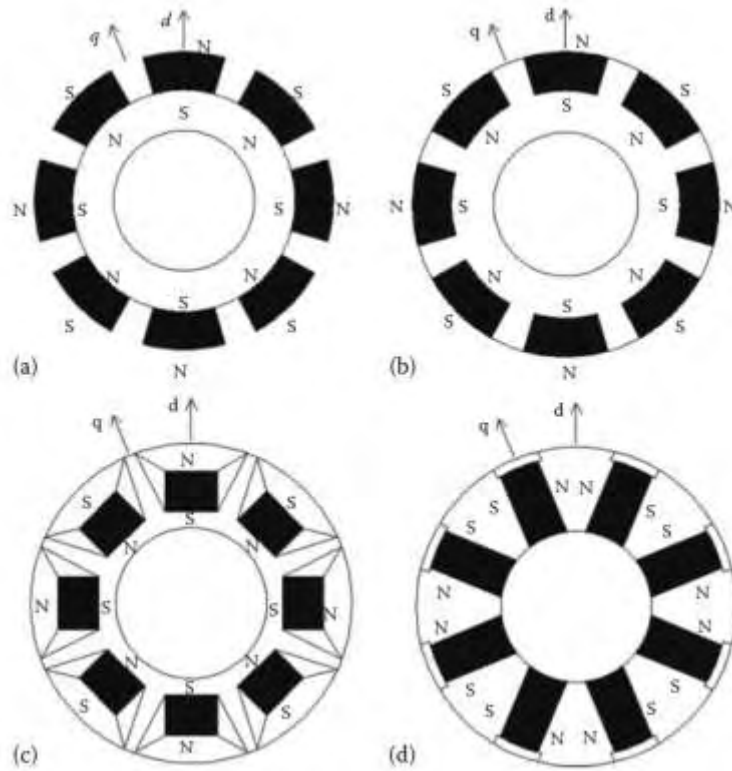


Figure 4.12: Permanent Magnet Rotor Types

- *Surface Mounted Topology*

In this topology, the magnets are mounted on the surface of the rotor periphery, as shown in Figure 4.12 (a). As can be easily understood, the greatest advantage of this machine is its ease and simplicity of construction and its small manufacturing costs in relation to other permanent magnet motors. In addition, this topology offers the highest air gap flux density since the magnet faces the air gap directly without interrupting any other material. A major disadvantage is that permanent magnets are exposed and special attention is needed when designing the motor in order to avoid demagnetization. Another drawback of such motors is that the permanent magnets are glued to the surface and, when the rotor rotates, receive great forces and there is a fear of detachment from the rotor body. Applications for this type of motors range from ship propellers to wind turbines.

- *Surface Inset Topology*

As the name suggests and as shown in Figure 4.12 (b), this type of machine has permanent magnets inside the rotor surface. This arrangement offers more mechanical strength compared to surface mount topology, as the magnets are completely and mechanically embedded in the rotor. In this case,

the danger of permanent magnets being demagnetized does not exist, but the iron between the magnets causes a torque opposite to the rotor movement.

- *Interior Topology*

In this case, the permanent magnets are not just inside the rotor surface but are placed deep inside the rotor body in holes that we have made either when cutting the sheet or when the rotor has become a solid body. It is clear that there are too many ways in which permanent magnets could be placed inside the rotor, and figure 4.12 (c) and (d) shows only two, the radial and circumferential configuration respectively. The internal magnet configuration is suitable for flux concentration and high power density. The reason is that too much of the magnet rotor's capacity is used in this case and therefore can be achieved high average magnetic induction of the air gap, and increased torque and power. Placing the magnets on the inside also gives a high torque to inertia in the rotor. In addition, this rotor topology has a high mechanical consistency and allows it to rotate at high angular speed. Also, the risk of demagnetization of permanent magnets is minimal and there is no risk of detachment of the magnets. On the other hand, the construction of such a motor is much more complex and expensive for both solid rotor and sheet metal, and in the both cases it takes a long time to create the openings.

- *Inner and Outer Rotor Topology*

The aforementioned inner rotor topologies can be applied to the outer rotor one. The placement of electric machines inside the wheels in vehicles reduces transmission losses in both propulsion and regenerative braking. When designing wheel motors it requires a special design as there is no transmission relationship involved. Torque requirements should be accurately calculated to allow the vehicle to start uphill and at the same time achieve the desired final speed. The outer rotor is beneficial because the centrifugal force tends to hold the magnets in place. The high moment of inertia also leads to a reduction in vibrations due to the harmonic torque smoothing. Another positive consideration is the possibility of integrating the motor into the vehicle wheel. Also, the absence of transmission offer reduced maintenance, higher reliability and efficiency and reduced weight. Complex cooling and reduced space for stator slots are the difficulties of such a configuration.

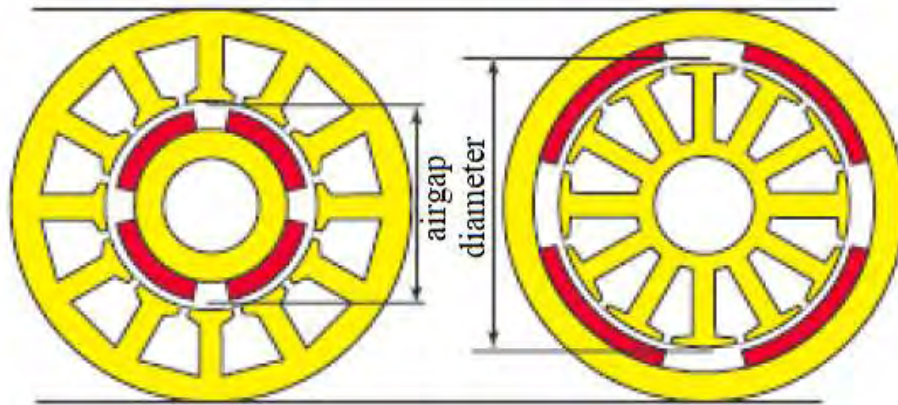


Figure 4.13: Machine with Inner rotor (left) and Outer rotor (right)

4.8 Winding

The winding types of the AC motors were analyzed in Chapter 3 of the induction motors. Specifically, the distributed and concentrated winding which permanent magnet brushless motors mainly use, were discussed in section 3.2.1.

In general, the PMSM (or BLAC) motor uses distributed winding, which offers sinusoidal air gap flux density distribution and the BLDC uses concentrated winding, which offers trapezoidal air gap flux density distribution.

4.9 Losses

The losses were discussed in Chapter 3 of the induction motors. There were analyzed the copper losses and the core losses. Core losses consist of two types, the hysteresis losses and the eddy currents losses.

In contrast to induction motors, the copper losses in permanent magnet brushless motors are much smaller because the rotor consists of permanent magnets rather than copper bars. Copper losses are therefore considered negligible.

4.10 Types of PM brushless motors

In this chapter two major Permanent Magnet Brushless motors will be presented, namely the Permanent Magnet Synchronous Motor and the Permanent Magnet Brushless DC. Nowadays, both motors and their drives are considered as a promising choice for electric propulsion.

4.11 Permanent Magnet Synchronous Motor

Permanent magnet synchronous motors (PMSM) or else permanent magnet brushless AC motors (BLAC) are used for high performance and high efficiency motor drives [11]. High performance motor control is defined by smooth movement across the entire speed range of the motor, full torque control at zero speed and quick acceleration and deceleration.

A PMSM reaction torque is created by the interaction of two magnetic fields (one on the stator and one on the rotor). The magnetic field of the stator is represented by the magnetic flux that is produced by stator's current. The magnetic field of the rotor is represented by the magnetic flux of permanent magnets, which is constant, except for the field weakening operation. These two magnetic fields are maximal when they are perpendicular to each other.

4.11.1 Principle of PMSM

The PMSM use distributed configuration of stator windings and have sinusoidal distribution of air gap flux. So the three-phase induced back electromotive force (BEMF) waveforms are given by:

$$e_a = E_m \sin(\omega t) \quad (4.19)$$

$$e_b = E_m \sin(\omega t - 120^\circ) \quad (4.20)$$

$$e_c = E_m \sin(\omega t - 240^\circ) \quad (4.21)$$

Where, E_m is the amplitude of back EMF waveforms and ω is the angular frequency. The relations of the three-phase sinusoidal currents are the follows:

$$i_a = I_m \sin(\omega t - \varphi) \quad (4.22)$$

$$i_b = I_m \sin(\omega t - 120^\circ - \varphi) \quad (4.23)$$

$$i_c = I_m \sin(\omega t - 240^\circ - \varphi) \quad (4.24)$$

Where, I_m is the amplitude of current waveforms and ϕ is the difference of the phase between the current EMF waveform and the back EMF waveform. Therefore, the converted electrical power is figured as:

$$P_e = e_a \cdot i_a + e_b \cdot i_b + e_c \cdot i_c = \frac{3}{2} E_m \cdot I_m \cdot \cos\phi \quad (4.25)$$

Consequently, the produced torque of the motor is expressed as:

$$T_e = \frac{P_e}{\omega_r} = \frac{3E_m \cdot I_m}{2 \cdot \omega_r} \cdot \cos\phi \quad (4.26)$$

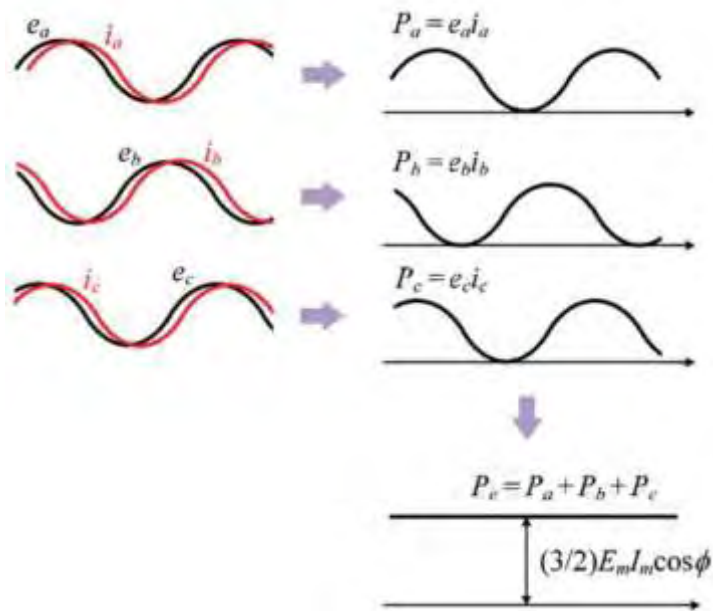


Figure 4.14: Produced Power of BLAC

4.11.2 Inverter of PMSM

PMSM and BLDC motor use the same inverter topology, namely the three phase full-bridge inverter as shown in Figure 4.15, but they have different switching schemes. Particularly, the PMSM use the pulse-width modulation (PWM) inverter, which have the same power inverter topology as the one used in the induction motor drive. Therefore, the PWM switching schemes that are widely used in PMSM drives are the hysteresis current control and space-vector modulation. These switching schemes were discussed in Chapter 3.4 of induction motor.

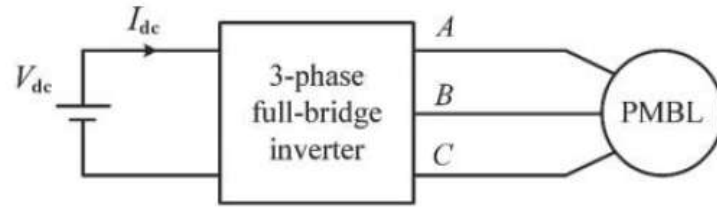


Figure 4.15: Three phase full-bridge inverter topology

4.11.3 Control of PMSM

The PMSM can adapt the control strategies that were mentioned for the induction motors in the third chapter. Field oriented control (FOC) has been widely used for EV propulsion and generally is more preferred from the direct torque control (DTC). In contrary to the induction motor, PMSM have to face permanent magnet's field excitation which is inherited by the magnets itself. That is the reason that makes the flux weakening control attractive. Another control strategy is the position sensorless control, offering the ability to remove the position encoder which is expensive.

- Field Oriented Control

The FOC strategy of the PMSM is the same strategy as the mentioned one for the induction motors in the third chapter, but here the torque is produced different. Considering the inertia J and friction B of the whole system, the motion equation is given as:

$$T_e = T_l + J \cdot \frac{d\omega_r}{dt} + B \cdot \omega_r \quad (4.27)$$

Where, T_l is the mechanical load torque.

- Flux-Weakening Control

The BEMF is proportional to the speed of the motor and air gap flux, leading to higher BEMF values. When BEMF exceeds drive's maximum output voltage, the PMSM is unable to draw current and therefore unable to produce torque. As a result, the rotor speed cannot be increased when the BEMF reaches an operating voltage threshold, unless the air gap flux is weakened. The required negative d-axis current increases the speed range, but due to a stator current limit, the applicable torque is reduced. The handling of the d-axis current into the motor has the desired effect of weakening the

rotor field, which reduces the BEMF voltage and allows the higher stator current to flow into the motor with the same voltage limit as the voltage of the DC link voltage.

- Position Sensorless Control

The PMSM generally requires a precise position sensor in order to implement control strategies. This position sensor is generally based on an optical encoder and most of the times it has high cost. For this reason, there has been development of position sensorless control. However, this technology is rarely used for EV propulsion because of the concerns about its precision and reliability.

4.12 Permanent Magnet Brushless DC Motor

Permanent magnet brushless DC motors (BLDC) have similar structure as the BLAC motor, having a three-phase armature stator winding and a rotor made from permanent magnet materials. However, the BLDC motor uses concentrated winding and has trapezoidal air gap flux density distribution compared to BLAC motor. Usually, the BLDC motor uses the surface mounted permanent magnet rotor topology, as shown in Figure 4.12 (a), because of the simple structure and control [7]. Again, the reaction torque is created by the interaction of the two magnetic fields produced by the stator and the rotor.

4.12.1 Principle of BLDC

As already mentioned, the BLDC motor uses concentrated winding in the stator with 120° coil span. The three phase BEMF waveforms are trapezoidal and the motor is fed by three phase rectangular currents. As shown in Figure 4.16, the power in each phase equals to $E_m \cdot I_m$ in the 120° conduction period. In the 60° of the non-conduction period the power equals to zero. Therefore, the electrical power is given by:

$$P_e = e_a \cdot i_a + e_b \cdot i_b + e_c \cdot i_c = 2 \cdot E_m \cdot I_m \quad (4.28)$$

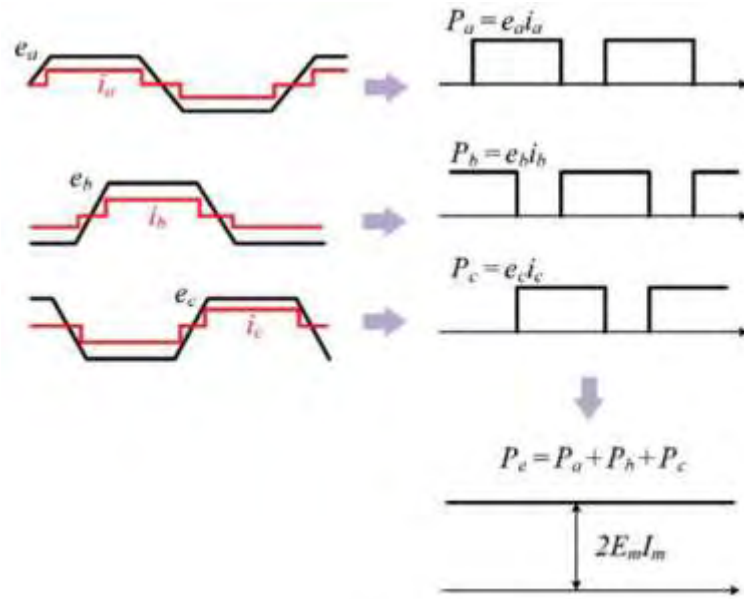


Figure 4.16: Produced Power of BLDC

So the produced torque is related as [14]:

$$T_e = \frac{P_e}{\omega_r} = \frac{2 \cdot E_m \cdot I_m}{\omega_r} \quad (4.29)$$

4.12.2 Inverter of BLDC

Two kinds of switching schemes are: the two phase 120° conduction scheme and the three phase 180° conduction scheme.

In the first scheme, the two phases are conducted in the period of 120° while the other phase is non-conducted. The BEMF-current waveform is almost rectangular. In the second scheme, the three phases are conducted in the period of 180°. The BEMF-current waveform is almost quasi square. Generally, the 180° scheme is more desired for constant power operations.

4.12.3 Control of BLDC

The BLDC motor can adapt the below control strategies.

- Phase Advance Angle Control

This strategy contributes in controlling the BLDC motor at high speeds, which is one of the main drawbacks of the motor. At high speeds, the phase current is not enabled fast enough in order to reach the desired value. For that reason, the advance of the turn on angle of the current phase, namely phase advance angle control, enable in time the phase current which change its value so it stays in phase with the BEMF in high speeds.

- Position Sensorless Control

This strategy is similar with the BLAC motors. However, BLDC motors do not require the precise rotor's position at any time, compared to BLAC motors, and usually they are working with Hall sensors or encoders which are simpler and less costly. That is the main reason this strategy is not so desired for BLDC motors.

4.12.4 Position Sensor for BLDC

The BLDC is driven by the three-phase inverter connected to the stator windings of the motor. This defines the phases of the motor being fed at each point in time according to the position of the rotor. This condition is necessary to produce a constant torque at a given speed. Since the rotor rotates synchronously with the field in the air gap, the position of the rotor can be determined by detecting the magnetic flux change [12]. Each phase induction voltage exhibits an ideal trapezoidal waveform with a flat region of 120° (electric degrees) per semi-permanent period, as shown in Figure 4.17.

In order to produce steady (with the minimum possible wavelength) electromagnetic torque, the intermittent operation of the BLDC power converter should be synchronized with the flat sectors of each induction voltage phase. For this purpose, the winding of each phase is activated twice within the period, and therefore six currents pass to the inter-converting elements of the inverter at 60° (electrical degrees) within the electrical period. This results in the generation of stator currents, which ideally have a rectangular waveform as shown in Figure 4.17. Therefore, it is necessary to know the position of the rotor every 60° in order to locate the flat sectors of each induction voltage phase. This information is obtained via "Hall" position sensors, optical encoders, or resolvers. In contrary, driving BLAC requires to know the rotor position at any time in order to produce the reference signals.

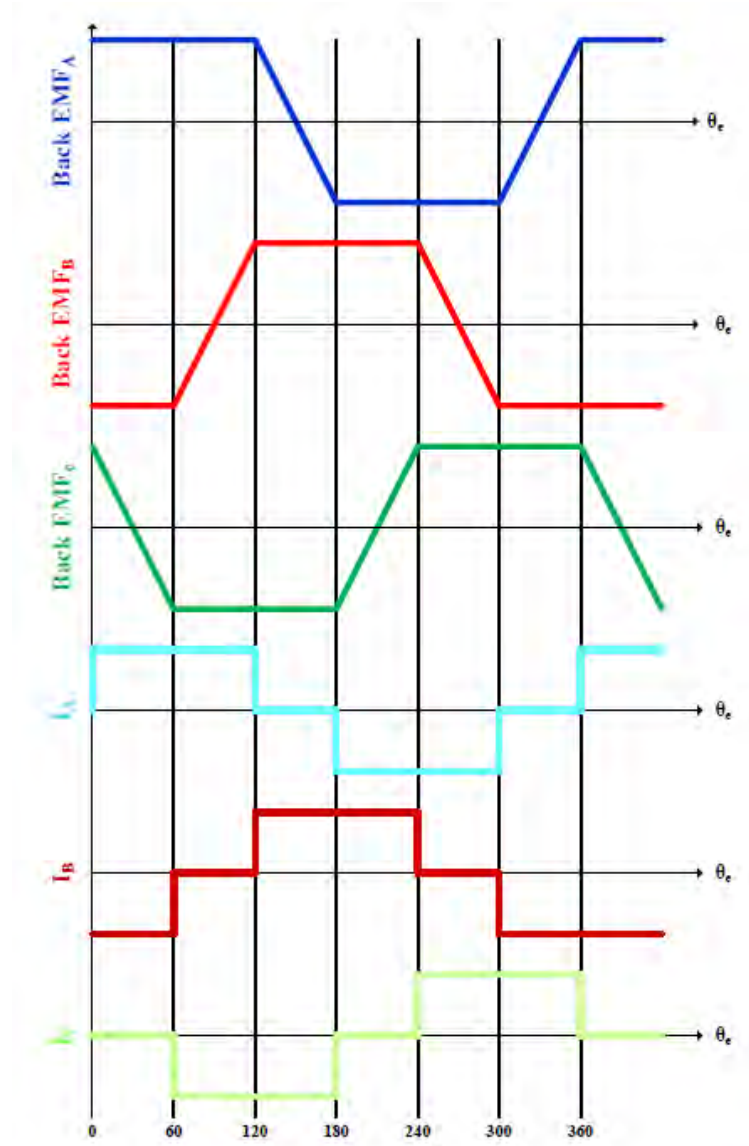


Figure 4.17: BLDC trapezoidal waveform

4.12.4.1 Hall Position Sensor

When a current conductor is placed into a magnetic field, a voltage is generated which is perpendicular to the current and to the magnetic field. This process is known as the “Hall effect”. When a perpendicular magnetic field is present, a Lorentz force is exerted on the current and disturbs its distribution, resulting in a potential difference. This voltage is the Hall voltage. Utilizing this phenomenon has led to the construction of homonymous sensors that detect the changes in the magnetic field. As the rotor rotation is synchronous with that of the magnetic field in the motor air gap, the Hall sensors, by detecting the changes in the magnetic field, can determine the position of the BLDC rotor. In particular, Hall sensors use a current conductor to detect the presence of a magnetic

field. They are actually triggered when a rotor's magnetic pole passes through their field of detection. In order to obtain safe conclusions about the position of the rotor at any time, it is necessary to use three Hall sensors placed at 120° electric degrees within the BLDC motor.

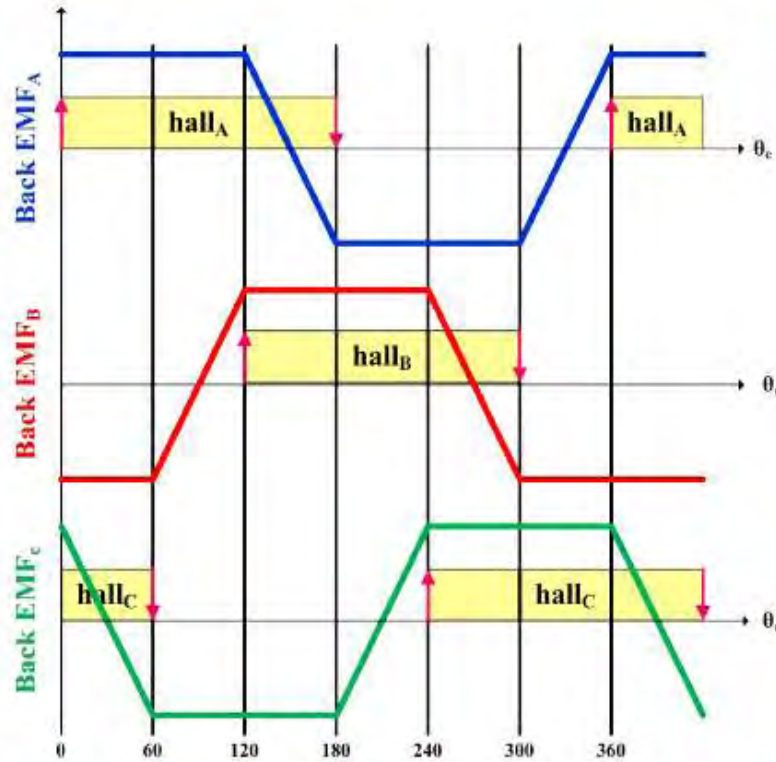


Figure 4.18: Trapezoidal waveform with hall sensors

4.12.4.2 Optical Encoder Position Sensor

This type of sensor uses the principles of optoelectronics to accurately determine the position of the BLDC rotor. As shown in the Figure 4.19, the optical encoder consists of a light source, a “light on” photocell, a perforated disk and a pulse boost circuit [12]. More specifically, a light emitting photodiode that is detected by a phototransistor is commonly used as a light source. The perforated disk is placed on the rotor to track its movement. Different materials, such as plastics, metals or even glass, are used to produce it. As shown in the Figure 4.19, on the disc side to the rotor, the light source is placed on the photocell on the other side of the disc to the stator.

The use of an optical encoder is not sufficient, as the position, rotation direction and rotor speed cannot be determined at any time. To address this issue, another optical analyzer is inserted within the BLDC motor, counter-diametrically from the first. This arrangement of optical analyzers allows

exploitation of the binary logic to extract the desired information, since when one photocell receives an infrared beam (1) the other receives nothing (0). The pulses that generate the two photocells have a phase difference of 90° , which is taken into account when combining the two signals.

The accuracy of this sensor in determining the position of the cursor depends on the number of holes in the optical disc. Obviously, the larger the holes the higher the accuracy of the measurement, for 360-hole optical discs, it is possible to determine the position of the rotor with the accuracy of 1° mechanical degree. High speed BLDC motors incorporate optical encoders with rotor positioning ability under 0.1° mechanical degree.

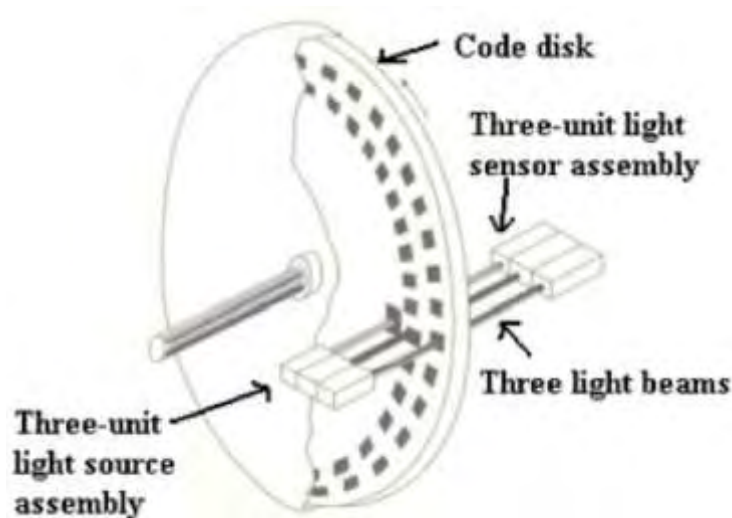


Figure 4.19: Optical encoder position sensor

4.13 Preliminary Design

The preliminary design of a motor provides a basic view of the required design of the motor. In Chapter 3 of induction motors a preliminary design had been carried out. The fundamental factors that were computed apply for the permanent magnet brushless motors. More specifically, the below fundamental factors were analyzed in section 3.7:

- Specific Magnetic Loading
- Specific Electric Loading
- Apparent Power
- Air Gap Voltage
- Current Density of the Winding

- Air Gap Surface
- Electromagnetic Torque
- Air Gap Thickness

In addition, field analysis can give a detailed magnetic field analysis and lead to confirmation of the motor characteristics expected by the preliminary design or to the need to improve it. The field analysis provides the distribution of the magnetic field and through it, with proper processing can be calculated with accurate magnitudes such as torque and power, losses, electric current density, as well as localized areas of the core that are in saturation. The content of section 3.8 applies to the permanent magnet brushless motors, in which are analytically discussed the below:

- Magneto-static problems
- Boundary Conditions
- The Finite Element Method
- Finite Element Analysis using the FEMM program

4.13.1 Field Factors

The field factors that must be taken into account during design are as follows:

- **Average Magnetic Induction of Air Gap**

Average magnetic induction of air gap is one of the essential factors of the design and is the magnetic motor load. Average magnetic induction of air gap is generally increased by increasing the dimensions of the magnet and decreasing the radial length of the gap. It also depends on the dimensions of the stator teeth.

The slope of the torque-ampere-turns motor curve is dependent on this medium, which increases with an increase in magnetic induction. Also, with a change in the average magnetic induction of air gap, the load value on which the motor is showing the maximum performance, as well as its value, is affected. Increasing the magnetic induction in the air gap increases the core losses and reduces the requirement in ampere-turns for a certain output power.

- **Magnetic Induction of Magnet under load**

In each case, a check is performed to ensure that the magnet is not at risk of demagnetization due to an external field. The surface magnet is weaker when its radial length is small.

- **Magnetic Induction Form**

The shape of the magnetic induction depends on the shape of the stator's teeth and the magnet's shape. Its knowledge is useful in driving the motor and evaluating the form and the harmonic content of the motor's back-EMF.

4.13.2 Performance

- **Performance curve**

The performance of the motor depends primarily on its electrical and magnetic load and its dimensions. The capacity of the motor to generate torque is linear with respect to the current in its windings except in the case where the iron core is in saturation. Therefore, changes in the dimensions of the stator teeth affect performance. To maximize the volume and magnetic properties of the motor core, its operating point should be shortly before saturation.

- **Maximum torque**

In any case, the possibility of achieving maximum torque at low speeds of rotation with a satisfactorily low current value should be guaranteed. The current flowing through the windings to the maximum torque demand is critical for the dimensioning of the power electronics used to drive the motor.

- **Heat Load of Turns**

The heat load of the winding depends on the performance of the motor as the windings flow from a different current to produce a certain torque for different torque generation capacities. The best use of the slot cross section is essential to reduce the current density.

4.13.3 Torque Ripple

The torque ripple is caused by many factors such as cogging torque, the interaction between the MMF and the air gap flux harmonics, or mechanical imbalances [9]. Torque ripple is generally undesirable as it causes vibrations and noise and may reduce the machine's lifetime. Extensive torque ripple may require measures such as skewing or machine geometry changes that may reduce the machine's overall performance.

The torque ripple is given from the relation:

$$T_{ripple} = \frac{T_{max} - T_{min}}{T_{mean}} = \frac{\Delta T}{T_{mean}} \quad (4.30)$$

Where, T_{max} is the maximum torque, T_{min} is the minimum torque and T_{mean} is the average torque. Obviously the smallest possible ripple torque is desirable.

4.13.4 Cogging Torque

There is an electromagnetic torque in permanent magnet motors even if the stator windings are not excited. This results from the interaction between the stator teeth and the rotor permanent magnet field. As the poles of the rotor line up with the teeth of the stator, the field around it changes, and a force is required to break the attraction. This force is referred to as cogging torque. Cogging torque is position dependent, according to the location of the stator teeth relative to the permanent magnets, as the magnets constantly search for a position of minimum reluctance.

In steady state the cogging torque appears as vibration and is therefore undesirable. Another consequence of the same phenomenon is the appearance of a harmonic component in the current of windings. Also, the cogging torque is added to the torque requirement when starting the motor. In particular, in permanent magnet motors with low output torque, the amplitude of the cogging torque may be a significant percentage of the total torque.

To reduce the cogging torque, the magnetic resistivity of the magnetic circuit must be partially removed at the rotation of the rotor. A design intervention is to find the dimensions of the magnet to be used to minimize the cogging torque. Another way to mitigate the effect of cogging is to select a fractional slot combination in which the number of stator slots divided by the number of rotor poles is a non integer number. As a result, only one side of the stator magnet lines up with the rotor slots. The

edges of the slots to not line up with the poles, which, reduces cogging torque. Finally, the most drastic measure is to construct the stator core with a skew to completely neutralize the cogging torque. This solution degrades the performance of the motor's performance and increases the manufacturing difficulty, so it only applies when the other actions to reduce the cogging torque are not sufficient.

The following index is used to compare the cogging torque to different types of machines [9]:

$$T_{cogging} [\%] = \frac{T_{max,cogging} - T_{min,cogging}}{T_{mean}} \cdot 100 = \frac{\Delta T_{cogging}}{T_{mean}} \cdot 100 \quad (4.31)$$

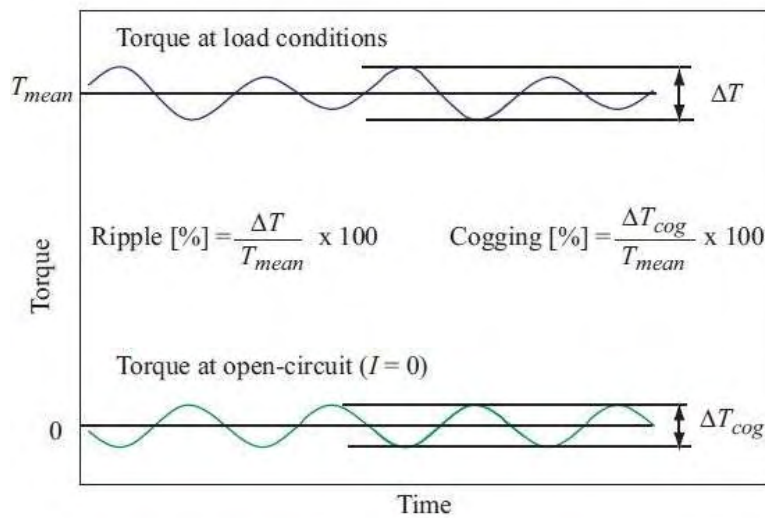


Figure 4.20: Definition of torque ripple and cogging torque

4.13.5 Short-circuiting Current

A very important factor in evaluating a machine is the stator current during a three phase short circuit. Until the motor protections (power electronics or relay) are activated, the machine windings will be subjected to currents with values more than twice the nominal. The smaller the short-circuit currents of a machine, the less insensitive the insulation of its windings, and therefore less maintenance is needed.

4.13.6 Resistance of Stator Windings

To calculate the resistance of stator windings, in the case the machine does not operate at 20°C, the temperature factor have to be used. For this reason the following formula is used:

$$r_{cu} = r_{cu,ref} \cdot [1 + \alpha \cdot (T - T_{ref})] \quad (4.32)$$

Where,

r_{cu} : Resistance in temperature “T”

$r_{cu,ref}$: Resistance in temperature 20 °C

T : Temperature factor for the material of the conductor (for copper is $3.9 \cdot 10^{-3}$)

T_{ref} : Operating temperature

The length of each coil is given from the relation:

$$l_{coil} = k \cdot (2 \cdot L + 2 \cdot l_{slot}) \quad (4.33)$$

Where,

l_{coil} : Length of each coil

k : Increment factor (usually equal to 1.2)

L : Active length of machine

l_{slot} : Length between two successive slots

Finally, the resistance per phase will be given by the following formula

$$R_{phase} = \frac{N \cdot Q_s}{m} \cdot r_{cu} \cdot \frac{l_{coil}}{A_{cu}} \quad (4.34)$$

Where,

R_{phase} : Resistance of stator windings per phase

N : Number of winding turns

Q_s : Total number of slots of machine

r_{cu} : Resistance in temperature “T”

l_{coil} : Length of each coil

A_{cu} : $A_{cu} = \frac{A_{slot} \cdot sff}{N}$ where, A_{slot} is the area of one slot and sff is the fill factor

4.13.7 Friction and Wind Losses

Friction and wind losses are usually neglected, especially in low speed applications. However, in high speed and low power applications, friction and wind losses are an important component of overall losses, with a significant influence on machine's performance. So they were approached through the following types:

Frictional losses are calculated from the empirical relationship [12]:

$$P_{fr} = \frac{K_{fb} \cdot (m_{motor} + m_{magnet}) \cdot rpm}{1000} \quad (4.35)$$

Where,

K_{fb} : Empirical factor

m_{motor} : Mass of rotor

m_{magnet} : Mass of magnets

rpm : The speed of rotation of the motor

Losses due to wind are estimated by the formula [12] [13]:

$$P_{windage} = \frac{L \cdot rpm \cdot (2 \cdot R_r + 2 \cdot B_m)^3}{10^6} \quad (4.36)$$

Where,

L : Active length of the motor

rpm : The speed of the motor

R_r : The outer radius of the motor

B_m : The thickness of the magnets

4.13.8 Calculation of Motor Efficiency Coefficient

For the calculation of the motor efficiency coefficient, the power output to the motor shaft must first be calculated. The calculation of the motor power output is made using the following relationship:

$$P_m = T_{mean} \cdot \omega_r \quad (4.37)$$

Where,

T_{mean} : The average torque

ω_r : The rotation speed of the motor (in rad/sec)

Therefore:

$$n = \frac{P_m}{P_{in}} = \frac{P_m}{P_m + P_{losses}} = \frac{P_m}{P_m + P_{cu} + P_{fe} + P_{windage} + P_{fr}} \quad (4.38)$$

Chapter 5

Conclusion

5.1 Conclusion

The specific diploma thesis aimed to study and analyze two categories of electric motors, the induction motors and the permanent magnet brushless motors. Specifically, were studied the squirrel cage induction motor (IM), the permanent magnet synchronous motor (PMSM or BLAC) and the permanent magnet brushless dc motor (BLDC). The background of electric vehicles and their drive systems were provided at the start. After that, both categories of electric motors were analyzed including their structure, operating principle, inverter topologies and control techniques. Permanent magnet brushless motors have smaller size, more compact structure and are more efficient compared to induction motors. In addition, they possess the ability to maintain full torque at low speeds. On the other hand, their cost is much higher than that of induction motors, mainly due to the use of permanent magnets. To conclude, both are very attractive options for the automotive industry and currently hold a large market share of electric vehicle motor drives, with the permanent magnet brushless motors having more potential and being more promising for the future.

5.2 Future Work

For future work is proposed a comprehensive design of the motors along with experimental measurement, in order to integrate them into a driving system for an electric vehicle. Ideally, a combination of the motors may result to an optimized outcome. For instance, a double motor topology could be beneficial, with the induction motor optimized for higher speed and low torque cruising while the permanent magnet motor could work well for low medium speed operation and high torque operation.

Bibliography

- [1] K. Laskaris and A. Kladas, “High Torque Internal Permanent Magnet Motor for Electric Traction Applications”, *Proceedings of the XVIII International Conference on Electrical Machines*, Vilamoura, Portugal, 6-9 September 2008, Paper ID 1428.
- [2] Κωνσταντίνος Λάσκαρης, *Σχεδιασμός και κατασκευή ηλεκτρικών κινητήρων μονίμων μαγνητών για ηλεκτρικά οχήματα*, Διδακτορική διατριβή, Αθήνα, ΕΜΠ, 2011.
- [3] K. Lalit and J. Shailendra, *Electric propulsion system for electric vehicular technology: A review*, Renewable and Sustainable Energy Reviews, 2014.
- [4] Husain Iqbal, *Electric and hybrid vehicles: design fundamentals*, New York, CRC Press, 2003.
- [5] Sandeep Dhameja, *Electric Vehicle Battery Systems*, Boston, 2001.
- [6] T. J. Pyrhonen and V. Hrabovcova, *Design of Rotating Electrical Machines*, Lappeenranta University of Technology, USA: John Wiley and Sons, 2008.
- [7] K. T. Chau, *Electric Vehicle Machines and Drives: Design, Analysis and Application*, International Research Centre for Electric Vehicles, The University of Hong Kong, 2015.
- [8] R. Krishnan, *Permanent Magnet Synchronous and Brushless DC Motor Drives*, Electrical and Computer Engineering Department Virginia Tech Blacksburg, Virginia, USA, 2010.
- [9] F. Meier, *Permanent-Magnet Synchronous Machines with Non-Overlapping Concentrated Windings for Low-Speed Direct-Drive Applications*, Stockholm: Royal Institute of Technology Department of Electrical Engineering Electrical Machines and Power Electronics, 2008.
- [10] Y.-K. Chin and J. Souldard, *Modeling of iron losses in permanent magnet synchronous motors with field-weakening capability for electric vehicles*, International Journal of Automotive Technology, Vol. 4, No. 2, pp. 87-94, 2003.
- [11] A. Hughes and W. Drury, *Electric Motors and Drives: Fundamental Types and Applications*, 2013.

[12] J. F. Gieras, *Permanent magnet motor technology : design and applications*, CRC Press 2010.

[13] K. Krishna Murty, *Equation For Windage Loss Of Axial Fflux, A.C. 3 Phase Synchronous Motor*, University of Central Florida.

[14] K.H. Nam, *AC Motor Control and Electric Vehicle Applications*, CRC Press, Boca Raton FL. 2010.